CENTRAL RESEARCH LIBRARY

ORNL/TM-5660

Cy 81

MARTIN MARIETTA ENERGY SYSTEMS LIBRARIES

3 4456 0250752 5

LWR Fuel Reprocessing and Recycle Program Quarterly Report for Period July 1 to September 30, 1976

B. L. Vondra

[redacted]

OAK RIDGE NATIONAL LABORATORY
CENTRAL RESEARCH LIBRARY
DOCUMENT COLLECTION
LIBRARY LOAN COPY
DO NOT TRANSFER TO ANOTHER PERSON
If you wish someone else to see this document, send in name with document and the library will arrange a loan.

OAK RIDGE NATIONAL LABORATORY
OPERATED BY UNION CARBIDE CORPORATION FOR THE ENERGY RESEARCH AND DEVELOPMENT ADMINISTRATION

This report was prepared as an account of work sponsored by the United States Government. Neither the United States nor the Energy Research and Development Administration/United States Nuclear Regulatory Commission, nor any of their employees, nor any of their contractors, subcontractors, or their employees, makes any warranty, express or implied, or assumes any legal liability or responsibility for the accuracy, completeness or usefulness of any information, apparatus, product or process disclosed, or represents that its use would not infringe privately owned rights.

ORNL/TM-5660

Contract No. W-7405-eng-26

LWR FUEL REPROCESSING AND RECYCLE PROGRAM
QUARTERLY REPORT FOR PERIOD JULY 1 TO SEPTEMBER 30, 1976

B. L. Vondra, Program Manager

Contributing Authors:

ORNL: W. D. Bond, C. H. Brown, D. O. Campbell, R. B. Fitts, J. H. Goode, W. S. Groenier, D. C. Hampson, J. C. Mailen, R. E. Moore, A. R. Olsen, O. K. Tallent, L. M. Toth, W. E. Unger, V. C. A. Vaughen, C. D. Watson, M. E. Whatley

ORGDP: E. H. Gift, J. H. Pashley, M. J. Stephenson

Date Published: November 1976

NOTICE This document contains information of a preliminary nature and was prepared primarily for internal use at the Oak Ridge National Laboratory. It is subject to revision or correction and therefore does not represent a final report.

OAK RIDGE NATIONAL LABORATORY
Oak Ridge, Tennessee 37830
operated by
UNION CARBIDE CORPORATION
for the
ENERGY RESEARCH AND DEVELOPMENT ADMINISTRATION

MARTIN MARIETTA ENERGY SYSTEMS LIBRARIES

3 4456 0250752 5

CONTENTS

Page

FOREWORD 1

SUMMARY. 2

1. ASSISTANCE IN SHEAR DEVELOPMENT AND RELATED PROBLEMS 4
   1.1 Introduction 4
   1.2 Summary 5
   1.3 Discussion 5
   1.4 Recommendations 11

2. HEAD-END STUDIES: VOLOXIDATION AND DISSOLUTION 13
   2.1 Voloxidation 13
      2.1.1 Studies of heat transfer in the rotary kiln 13
      2.1.2 Studies of residence time distribution in the rotary kiln 18
      2.1.3 Component development 23
   2.2 Hot-Cell Studies 23
      2.2.1 Hot-cell dissolution 26
      2.2.2 Radioactivity in off-gas 29
      2.2.3 Insoluble dissolution residue 33
      2.2.4 Plutonium extraction into 30% TBP 38
      2.2.5 Solution stability 42
      2.2.6 Characterization methods 45
   2.3 Building 4507 Hot-Cell Operations 46
      2.3.1 Development of in-cell equipment 46
      2.3.2 Decommissioning the CRF 46
      2.3.3 Miscellaneous 47

3. PUREX PROCESS STUDIES (SOLVENT EXTRACTION) 53
   3.1 Laboratory Studies 53
      3.1.1 Solvent cleanup 53
      3.1.2 Plutonium valence adjustment 58
      3.1.3 Ruthenium chemistry 59
      3.1.4 Chemistry of hydroxylamine and hydrazine in the reductive stripping of plutonium 60
      3.1.5 Plutonium extraction studies 68
   3.2 Purex Studies with Irradiated Fuels 68
      3.2.1 Purex process studies 69
      3.2.2 Solvent extraction flowsheet development 73
   3.3 Cold Studies 74
      3.3.1 Mixer-settler extraction studies 74
      3.3.2 Batch countercurrent extraction studies 75

Page

4. OFF-GASES - FLUOROCARBON ABSORPTION STUDIES 79
   4.1 Fluorocarbon Absorption Process Development 79
      4.1.1 Pilot-plant operation 79
      4.1.2 Process application 82
   4.2 Chemical Studies of Contaminants in LWR Off-Gas Processing 85
   4.3 Reliability Studies 86
   4.4 Engineering Design Criteria Studies 88

5. FINISHING PROCESSES - MOX FUEL FABRICATION 89
   5.1 MOX Fabrication Processes 89
   5.2 MOX Fabrication Facilities 90
      5.2.1 Effects of plutonium radiation characteristics on containment criteria 90
      5.2.2 Remote manipulator and viewing development 90
      5.2.3 Development of the powder conveying system 91

6. URANIUM HEXAFLUORIDE CONVERSION 92

7. ECONOMIC STUDIES 93
   7.1 LWR Recycle Data 93
   7.2 Financial Study 102
   7.3 Program Review 102

8. RADIOLOGICAL TECHNIQUES FOR ENVIRONMENTAL IMPACT ASSESSMENTS OF THE LWR FUEL CYCLE 105
   8.1 Introduction 105
   8.2 Effect of Building Structures on Radiation Exposure Pathways 105
   8.3 Model for Internal Dose Protection Factor 106
   8.4 Model for External Dose Protection Factor 108
   8.5 Implementation of the Models for Dose-Rate Protection Factors 109
      8.5.1 Internal dose 109
      8.5.2 External dose from airborne radionuclides 110
      8.5.3 External dose from surface-deposited radionuclides. 111
   8.6 Limitations of the Model 113
   8.7 Progress to Date and Future Plans 114

9. REFERENCES 115

LIST OF TABLES

		Page
Table 1.	Some commonality problems in the head-end processing of spent LWR and LMFBR fuels	6
Table 2.	Experimental conditions for the RTD tests (6-in.-diam pipe)	20
Table 3.	^{129}I distribution during fuel dissolution	29
Table 4.	Effect of duration of air sparge on ^{129}I content of dissolver solution	30
Table 5.	^{14}C distribution during fuel dissolution	31
Table 6.	Calculated and observed radioisotope concentrations in dissolver solutions (March 16, 1976)	34
Table 7.	Distribution of radioisotopes during dissolution in run 2 (212 g of uranium)	36
Table 8.	Distribution of radioisotopes during dissolution in run 4 (314 g of uranium)	37
Table 9.	Mass analysis of actinides from run 2	39
Table 10.	Effectiveness of macroreticular resins in adsorbing plutonium from simulated Purex solvent	56
Table 11.	LWR hot-cell Purex solution flows	71
Table 12.	Times required to reach 90 to 99.9% of steady state in mixer-settlers	72
Table 13.	Flow ratios and concentrations calculated by SEPHIS	73
Table 14.	Comparison of experimental distribution of uranium and HNO_3 with values calculated by the SEPHIS code	77
Table 15.	Countercurrent extraction of zirconium from simulated fission products	78
Table 16.	BWR fuel needs for self-generated plutonium recycle of a reload region initially discharged at 13,519 MWd/MT	94
Table 17.	BWR fuel needs for self-generated plutonium recycle of a reload region initially discharged at 17,574 MWd/MT	96

		Page
Table 18.	BWR fuel needs for self-generated plutonium recycle of a reload region initially discharged at 21,832 MWd/MT	98
Table 19.	BWR fuel needs for self-generated plutonium recycle of a reload region initially discharged at 27,037 MWd/MT	100
Table 20.	Capitalization by companies (Petroleum industry)	103
Table 21.	Capitalization by companies (Nuclear reactor suppliers)	104
Table 22.	Capitalization by industry	104

LIST OF FIGURES

Figure		Page
1	Typical temperature profile in the kiln.	17
2	Residence time distribution data obtained using a 6-in.-diam, 7.0-ft-long rotating pipe.	22
3	Plutonium extraction behavior from feed prepared by dissolution of irradiated UO_2. Feed adjusted to 3 M HNO_3 was contacted with equal volumes of 30% TBP--dodecane. UO_2 fuel: Assembly B05, Carolina Power and Light H. B. Robinson reactor fuel irradiated to 31,360 MWd/metric ton.	41
4	Work tray and fuel storage wells for voloxidation cell.	49
5	Partially assembled work tray and fuel storage wells, showing bolted construction and cell exhaust plenum and HEPA filter.	50
6	Intercell transfer port.	51
7	Intercell transfer port with manipulator-operated door in open position.	52
8	Purex process (preliminary hot-cell flowsheet).	70
9	Summary of recent pilot-plant tests with krypton, xenon, and carbon dioxide (9.0-foot absorber column, 300 psig, and 0°F).	81
10	Calculated cold trap removals of various feed gas components as a function of trap temperature.	83

FOREWORD

Eight tasks under the LWR Fuel Reprocessing and Recycle Program have been assigned to UCC-ND with major efforts centered at the Oak Ridge National Laboratory. Because of the close relationship of the reprocessing activities with the on-going LMFBR Fuel Reprocessing Program at ORNL, those tasks will be managed within a combined LWR/LMFBR Fuel Reprocessing Program under the direction of W. D. Burch, Program Director. B. L. Vondra, as LWR Program Manager, will coordinate all activities reported here. Responsibility for the coordination and collation of reports of all work at Oak Ridge was assigned to ORNL by SRO/SRL, who is designated as the lead organization for the LWR Fuel Recycle Program.

Projects for which budget and work plans have been established are as follows:

F-OR-02-001	SRO/LWR:	Assistance in Shear Development and Related Problems
F-OR-02-002	SRO/LWR:	Head-End Studies: Voloxidation and Dissolution
F-OR-02-003	SRO/LWR:	Off-Gases Fluorocarbon Absorption Studies
F-OR-02-004	SRO/LWR:	Purex Process Studies (Solvent Extraction)
F-OR-02-005	SRO/LWR:	Finishing Processes - MOX Fuel Fabrication
F-OR-02-006	SRO/LWR:	Uranium Hexafluoride Conversion
F-OR-02-007	SRO/LWR:	Economic Studies
F-OR-02-008	SRO/LWR:	Radiological Techniques for Environmental Assessments of the LWR Fuel Cycle

SUMMARY

This is the third quarterly report issued on the LWR Fuel Reprocessing and Recycle Program at ORNL as part of the national program administered by Savannah River Operations - Savannah River Laboratory.

Two additional dissolutions were made using irradiated fuel for the H. B. Robinson II reactor. Characterization of the solids has been continued, and results to date are reported.

An extension of time was given for the preparation of bid proposals for the design and fabrication of a model 1/2-ton/day voloxidizer. The extended due date is October 15, 1976.

Preliminary heat transfer tests of a rotary kiln voloxidizer were completed. These tests, along with additional planned investigations, should serve as a basis for evaluating mathematical models for the operation of the kiln and help establish the relative importance of various possible heat transfer mechanisms.

Tests of the residence time distribution of material in various diameter kilns were initiated by measuring residence times in a 6-in.-diam tube; the results were in agreement with those obtained in a previous test with a commercial kiln.

The remaining fluorocarbon absorption process pilot-plant tests scheduled under campaign 3 have been completed. Analysis of the data show that greater than 99.99% of the carbon dioxide and xenon impurities were removed. Process modeling studies are continuing.

Chemical studies of stainless steel corrosion by R-12 solutions in the presence of iodine and water are continuing. Methyl iodide was found to be miscible in R-12.

The final report by Kaman Sciences on process reliability has been issued.

An ORNL/SRL survey study was made of commercial and potential spent light-water reactor (LWR) fuel reprocessors to identify unresolved shearing and related head-end problems. Areas of difficulty were categorized broadly by four groupings: (A) mechanical technology, (B) safety technology, (C) waste disposal, and (D) a pressing need for an LWR fuel Reference Information Center. Past reprocessing head-end experience in the United States indicated that a new hot-cell domestic shearing system must be developed, and that remote operability and maintenance must be demonstrated at high throughputs. As a result of the study, several research and development program tasks to solve the principal problems will be prepared for consideration and review early in FY 1977.

1. ASSISTANCE IN SHEAR DEVELOPMENT AND RELATED PROBLEMS

C. D. Watson (Chemical Technology Division, ORNL) and
S. Dyer Harris (Savannah River Laboratory)

1.1 Introduction

An ORNL/SRL study was made to identify problems associated with the head-end processing of LWR fuels and to provide a basis for the necessary research and development programs to solve them. The primary method of inquiry was by direct contact with commercial reprocessors or potential reprocessors so that their thoughts and experience on head-end problems could receive appropriate attention in the scoping of future research and development programs.

In general, experience in the United States with the reprocessing of spent LWR fuels is limited to that of Nuclear Fuel Services, Inc. (NFS), West Valley, New York. Contact with reprocessors abroad, notably licensees of St. Gobain Nucleaire, was not successful owing to proprietary restrictions and limitations. However, the experience of ORNL with shear development,[1] the current, related efforts at ORNL in fast breeder reactor fuel (LMFBR) reprocessing, and the willingness of other domestic reprocessing interests to discuss their problems allow a candid view of the status of shearing and related head-end technology problems to be established. The inquiry included all aspects of head-end operations between the introduction of spent fuel assemblies into the mechanical processing cell and their delivery as sheared segments to the downstream voloxidation or dissolution step.

1.2 Summary

The need for new and advanced developmental work in several head-end areas was recognized by all individuals interviewed. Everyone basically agreed that a new head-end shear system should be developed. The paramount thought in all the discussions included the basic theme that the Shear Development and Related Problems research and development programs should be structured in such a manner that the resulting technology would provide the appropriate necessary proof and support for the ready licensing of later commercial equipment and attendant facilities. Differences of opinion were chiefly concerned with the level of Federal support and participation in solving problems and demonstrating concepts. For orientation purposes, some common problem areas in the head-end processing of LWR and LMFBR fuels are summarized in Table 1.

The specific LWR problems areas that were identified can be grouped broadly into four headings: (A) mechanical technology, (B) safety technology, (C) waste disposal, and (D) information needs. Under each of these can be listed more specific items, some of which are generic to head-end processing, and some of which may be peculiar to specific head-end designs.

1.3 Discussion

A brief discussion of each of the four categories of LWR problem areas is given below. This information will be expanded upon and included in a topical report on the shear program which is scheduled for release in the first half of FY 1977.

Table 1. Some commonality problems in the head-end processing of spent LWR and LMFBR fuels

Problem area	LWR	LMFBR
1. Mechanical		
A. New shear system development and evaluation	✓	✓
B. Disassembly desired	?	✓, ?[a]
C. Cropping of unfueled portions of subassemblies	✓	✓
D. Fuel feeding and withdrawal system needed	✓	✓
E. Quantitative transport of sheared product	✓	✓
2. Containment		
A. Sheared fuel particulates, volatile fission products and gases	✓	✓
B. Mechanical seal development and control of internal shear environment	✓	✓
3. Safety and Hazards		
A. Handling of Zircaloy and Zircaloy fines	✓	X
B. Handling of sodium and sodium corrosion	X	✓
C. Decay heat dissipation	✓[b]	✓
D. Criticality aspects	?[c]	✓
E. Fire fighting	✓	✓
F. Seismic analysis in relation to equipment size and weight and facility aspects	✓	✓
4. Waste Disposal		
A. Densification of hulls and end adaptors, flattening, briquetting, melting	✓[d]	✓
B. Shipping of densified product	✓	✓
5. Systems analysis and control		
A. Computer and microprocessor	✓	✓
B. Update ORIGEN[e] code (heat, curies, radionuclides, mass)	✓	✓

[a]Shroud is difficult to shear and process.
[b]Assumes fuel is not long decayed.
[c]Minor compared to LMFBR.
[d]Probably much more difficult than LMFBR.
[e]See ref. 2.

A. Mechanical Technology

1. Demonstrate hot-cell shearing device at high throughput

Existing shears in this country are based on ORNL developments that were essentially discontinued in 1964.[1] Shears developed abroad (England, France), based on the U.S. shear, appear to operate as intended, but the technology is not available.

In summary, there is no extensive, sustained experience in this country on which to base an extrapolation of shear operation to demonstrated commercial rates of up to 10 metric tons of spent fuel per day. One possible solution is to operate one or more shears of the ORNL type in parallel. At this time, no complete characterizations exist of a shear feeder, gag shape, gag pressures, blade shapes, blade wear, chute and stacking characteristics, powder flow, particle and dust production, or the adaptation or adjustments required for ductile or brittle fuels. Sheared product, both ductile and brittle, must be characterized to ensure desired reproducible properties for subsequent voloxidation dissolution steps. Stand-in materials were tested at ORNL to mockup both short- and long-exposure fuels. It was found that brittle material sheared into suitable small pieces for satisfactory processing. Ductile materials tended to deform rather than shear cleanly, partially closing the ends of the sheared pieces. Partially closed ends inhibit evolution of tritium and other volatile fission products and retard dissolution. Development and demonstration of a production-type shear incorporating improvements suggested above would be the most positive way of preventing problems with this critical item. Programs at ORNL and elsewhere to discover alternatives to shear-leach for penetrating or segmenting cladding should also be encouraged and pursued intensively.

2. Dry lubrication for in-cell mechanical components

Commercial spent fuel reprocessing experience using organic greases for lubrication of mechanical in-cell moving parts was poor. In the shear, ionizing radiation caused early breakdown of the lubricating qualities of greases. Remote addition of lubrication was time-consuming and difficult. Excessive greasing of bearing surfaces in the shear head tended to cause chemical contamination of the subsequent Purex solvent extraction processing steps. Major advances in dry lubrication have been made in both dry material lubricants and gas lubrication techniques. Where possible, this technology should be transferred to head-end machinery to alleviate the problems listed above.

3. Material balance methods and instrumentation for interrogation and control

Reliable in-line instrumentation for interrogation and control of process streams is essential for safe operation, material accountability, and conformance to regulations. Computer analysis and microprocessors should be utilized to provide control and real-time analysis of process variables.

4. Seals for cell wall penetrations and process equipment connections

The penetration of hot-cell walls up to 6 ft thick by rotating or reciprocating shafts, process liquids and gaseous lines, instrumentation lines, and other transmission devices, etc., present serious confinement design problems. As the environmental tolerance release level for various radionuclides to the environment is reduced by factor(s) of 10 or more, the penetration and sealing of shield walls technology must be updated, evaluated, and reestablished accordingly.

5. Control of cell atmosphere

As the burnup of LWR fuels increases, the decay heat along with heat from lights, crane motors, processing vessels, etc., must be removed to maintain the cell at some predetermined desirable operating level (100 to 120°F).

The humidity, oxygen content, and volatile fission products will require close control, removal, and disposal. Fire-fighting measures further complicate cell atmosphere control.

B. Safety Technology

As mentioned earlier in the summary, a study group should be established to determine the type and extent of containment structure required for the head-end plant as well as the distance it should extend downstream.

1. Fire control methods

The pyrophoricity of Zircaloy and uranium metal fines presents operational problems in the mechanical head-end and dissolution operations.

Existing and proposed shear-leach processes should be examined very closely to identify points where pyrophoric hazards exist. Typically, these conditions might consist of friction heating between shear blades, "wiping" of Zircaloy between the blades, accumulations of fines, wet-dry cycling of fines, or exposure to excess oxygen and decay heating. Results from experiments that simulate these hazards, along with various fire control devices, would be generally useful in designing or updating head-end facilities.

2. Confinement and collection of volatile fission products

Noxious components must be isolated from the shear cell ventilation off-gas before it is released to the environment. The primary gases of

concern are I, ^{3}H, ^{85}K, and ^{14}C. Generally, iodine and particulates are removed in existing plants by caustic scrub, filtration, or a combination of these operations.

3. Criticality and radiation hazards

These hazards are normally peculiar to the specific design of a reprocessing facility. Two areas that may be common to all proposed facilities and would, therefore, benefit from a basic study are: (1) criticality of a fuel assembly in the shear, and (2) criticality of sheared fragments in discharge chutes and dissolver buckets.

4. Decay heat removal from fuel

State-of-the-art information available for heat transfer from irradiated LWR rod bundles in air or held in clamping devices and other mechanical processing equipment is incomplete. At ORNL, development was begun,[3] but soon discontinued, of a computer code to calculate heat transfer from the various spent LWR fuel configurations in air.

5. Fault-tree analysis

A fault-tree analysis of a mechanical head-end facility containing a shear and other cropping/disassembly equipment has not been made in the past. This type of analysis is essential in the design and operation of new head-ends in that a series of events, possibly including a fire, could trigger an unexpected phenomenon that would endanger the operators, facility, and biological surroundings.

C. Waste Disposal

A head-end facility in which spent LWR fuel is cropped (or disassembled) and sheared will generate significant quantities of unfueled metal waste.

For each metric ton of fuel processed, approximately 0.4 of a metric ton of metal (Zircaloy, Inconel, stainless steel, etc.), including the cladding hulls from the dissolver, will have to be processed and stored. Essentially no work has been done in this field, and commercial spokesmen recommend that such a problem be pursued in a separate, aggressive type of research and development program.

D. Information Needs

It is very difficult to obtain drawings and reliable physical data on the various sizes, configurations, etc., of PWR and BWR fuels. Our study was handicapped by the paucity of drawings and the available information. It is apparent now that the LWR shearing development and related head-end programs must have a constantly updated information center from which data generated by both ERDA and commercial sources can be dispensed. Such a center must be operated so that programmatic needs can be met without compromising proprietary information.

1.4 Recommendations

Based upon the above summary, it was concluded that additional work is required as outlined below.

A. Mechanical Technology

1. Demonstrate remote operability and maintenance of a new hot-cell shear system at high throughputs.
2. Evaluate and develop dry lubrication methods for in-cell mechanical components.
3. Develop material balance and interrogation methods.

4. Evaluate alternative means for acceptable cell wall penetrations for transmitting power (both mechanical and electrical).
5. Develop and evaluate methods for the control of the shear system environment and the cell atmosphere.

B. Safety Technology

1. Study and evaluate in-cell fire control methods.
2. Evaluate confinement and collection techniques for volatile fission products, off-gases, and particulates.
3. Analyze criticality and radiation hazards.
4. Analyze decay-heat removal from spent fuel under normal and abortive processing conditions.
5. Perform a fault-tree analysis of head-end systems.

C. Waste Disposal

1. Study densification of hulls and end adapters, flattening, briquetting, and melting.
2. Evaluate the needs relative to the shipping of densified product.

D. Information Needs

1. Collect, at one center, available information on shear systems technology.
2. Collect, at one center, physical descriptions of existing and planned boiling water reactor and pressurized water reactor fuel assemblies.

2. HEAD-END STUDIES: VOLOXIDATION AND DISSOLUTION

2.1 Voloxidation

D. C. Hampson and M. E. Whatley (Chemical Technology Division, ORNL)

The voloxidation process is currently being developed as a head-end method for removing tritium from the fuel prior to aqueous processing. Based on experimental work, it appears that this objective can be met by heating the oxide fuel to about 450°C in flowing oxygen or air. Volatilization of tritium and, to a lesser extent, some of the other fission products is effected as the UO_2 becomes restructured during oxidation to U_3O_8. Early removal of tritium from the fuel into a relatively small volume is desirable to avoid extensive dilution of the tritium with water in the subsequent fuel dissolution step.

During this report period, the investigation of the applicability of rotary kilns for the voloxidation process was continued by initiating tests that will extend residence time distribution studies to include kiln tubes of various diameter, and by the performance of preliminary heat transfer tests using a commercial kiln.

2.1.1 Studies of heat transfer in the rotary kiln

W. S. Groenier, C. H. Brown, and M. E. Whatley (Chemical Technology Division, ORNL)

The type of equipment being considered for the voloxidation process is a rotary kiln to which the sheared fuel is fed continuously and oxidized from UO_2 to U_3O_8. During the oxidation, which is generally accompanied by pulverization, a large fraction of the tritium should be released to a filtered off-gas system.

Although rotary kilns have been used commercially for many years, the literature contains very little definitive data that can be used for design purposes. We have initiated a study of heat transfer in rotary kilns that should describe, through the application of previously developed heat transfer data correlating methods, the fundamental modes of heat transfer and the influence of particle residence time distribution, or dispersion, on these phenomena. Applications of the study results may strongly influence kiln design in such important areas as lengths and separation of heating and cooling zones. Initial investigations are described below. Additional tests are planned for the near future. The data collected will serve as a basis for evaluating mathematical models of the operation of the kiln and will help establish the relative importance of the various heat transfer mechanisms.

Heat transfer in rotary kilns can proceed by several mechanisms, the most important of which include conduction between the charge and the kiln wall, radiation from (or to) the kiln wall, convective or dispersive movement of the charge, and conduction and convection by the gas phase. The various mechanisms assume different degrees of importance, depending on the local conditions within the kiln. Conduction is important whenever a significant temperature difference exists between the charge and the wall. Radiation is important only in areas where temperatures are fairly high (greater than $\sim$ 480 K),[4] such as in the heating zone. In cases where a steep axial temperature gradient is imposed, the analysis of heat transfer data becomes more complicated. It is here that the charge at one point in the kiln can "see" a range of kiln wall temperatures and that convective transport, caused by the dispersion of material resulting from

the tumbling (rotating) action of the kiln, becomes important. Convective heat transport is manifest in the form of an effective axial thermal conductivity and may comprise the predominant mode of heat transfer. Heat transfer via the gas phase is generally thought to be of secondary importance when net flow rates of gas are small; however, it could also have a significant effect in a high axial temperature gradient.

The recent preliminary heat transfer tests were conducted mainly to study the cooling zone since it may be desirable for the voloxidizer to feed the fuel charge directly to a dissolver. Temperatures were also measured in the heating zone. These tests were performed in a 6.5-in. (0.17-m)-diam x 7.5-ft (2.29-m)-long rotary kiln manufactured by the C. E. Bartlett and Snow Company. This experimental apparatus has been described in an earlier report.[5]

Experimental procedure. Steady-state heat transfer rates were measured in the kiln for several combinations of kiln slope, solids flow rate, furnace temperature, and cooling water flow rate. No gas was passed through the kiln during any of the tests. The following temperature measurements were made during each test: (1) temperature of the outer surface of the kiln at five positions in the furnace zone and three positions in the cooling zone, (2) temperature of the cooling water in and out of the water-spray cooler, and (3) average temperature of the solids bed at several positions along the axis of the kiln from near the feed entrance to near the product exit point. The solids-bed temperatures were monitored via a movable cup containing a thermocouple which could be positioned at any point along the axis of the kiln. The cup was turned in such a way that a batch of solids was held and the temperature

was monitored on a recorder. Several batches were caught and dumped until a steady temperature was observed. The solids flow rate through the kiln and the water flow rate to the water-spray cooler were also measured.

Essentially the same procedure was followed in each run. The temperature controllers on the kiln furnace were set at the desired levels, and the kiln tube was allowed to reach a steady temperature. Then the rotational speed of the kiln and the water flow rate to the spray cooler were set at the desired values. Material was fed to the kiln at the desired rate until a steady flow of material out of the kiln was established and the solids-bed temperatures had stabilized. At this point, the temperature and flow rate measurements described above were made and the equipment was shut down.

Fourteen heat transfer runs were made using this technique. The prototype fuel feed material used in each of the tests was 1/4-in. (0.00635-m)-diam, 1-in. (0.0254-m)-long porcelain-filled stainless steel tubing. An analysis of the feed material showed it to consist of 32 wt % porcelain cylinders, 61 wt % stainless steel tubing, and 7 wt % porcelain fines. Tests were made at two different kiln slopes, 0.097 in./ft (0.0081 m/m) and 0.22 in./ft (0.018 m/m), three rotational speeds from 0.033 to 0.13 rps, solids flow rates from 1.05 to 2.55 kg/sec, cooling water flow rates from 0.022 to 0.098 kg/sec, and nominal furnace zone temperatures from 798 to 958 K.

Experimental results. A typical temperature profile for the kiln is presented in Fig. 1, where the temperatures of the outer surface of the kiln are shown as a function of the distance from the feed point. The kiln surface temperature in the region between the furnace and the cooling zone was not measured since this zone was not equipped with thermocouples.

ORNL DWG. 76-14566

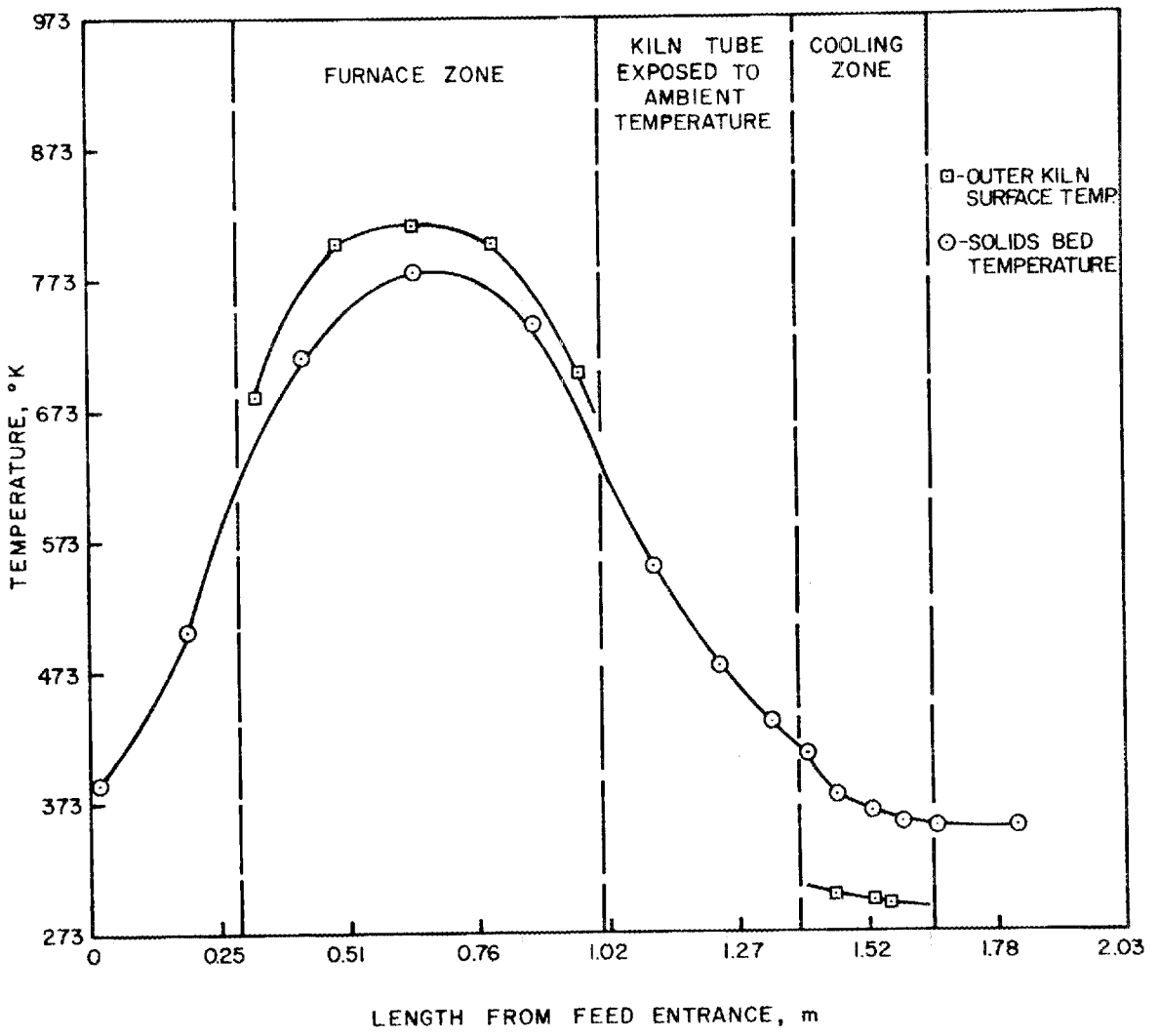

Fig. 1. Typical temperature profile in the kiln.

As expected, the surface temperature of the kiln in the furnace zone is not isothermal because of heat losses from the ends of the furnace. Also shown are the solids-bed temperatures as a function of distance from the feed point. It is interesting to note that the solids-bed temperature decreased significantly in the zone between the furnace and the water-spray cooler where the kiln is cooled by external convection, and possibly by conduction to the cooling zone, to ambient temperature. A detailed analysis of these, and other, data will be made as tests continue.

2.1.2 Studies of residence time distribution in the rotary kiln

W. S. Groenier, T. D. Welch, and M. E. Whatley (Chemical Technology Division, ORNL)

The residence time distribution (RTD) of process material in the kiln must be known in order to accurately predict kiln performance for design purposes. The kiln could be characterized as a plug flow system if all particles had the same residence time. In actual practice, however, significant deviations from idealized plug flow occur, and there is a distribution or range of particle residence times. The RTD can be compared to axial dispersion occurring in a tubular gas-liquid or liquid-liquid reactor. The amount of tritium removed from sheared fuel by the voloxidation process will require knowledge of the RTD in the kiln as well as reaction rate information.

The purposes of current tests are to extend the results of a previous study, where the RTD was measured for a commercial kiln, and to determine the influence of kiln diameter on the RTD using several rotating pipes of

different diameter. Initial work has been carried out in a 6-in. (0.15-m)-diam tube to verify the previous results. Additional RTD tests will include the use of a larger, 18-in. (0.46-m)-diam tube.

The experimental equipment consists of a vibratory feeder which continuously feeds 1-in.-long sheared prototype fuel into a 6-in. (0.15-m)-diam, 7-ft (2.13-m)-long rotating pipe containing six equally spaced 1-in. (0.025-m)-wide axial flights to lift and tumble the sheared fuel. The pipe rests on a set of rollers that are powered by a 1/4-hp variable-speed electric motor. Feed rate, rotational speed, and drum slope may be varied.

The stimulus-response procedure used has been described previously.[6] Basically, the method consists of introducing a step change of tracer in the feed and measuring the weight fraction of tracer in the product as a function of time.

Six tests using this 6-in.-diam pipe were performed. All runs were made with a slope of 1/4 in./ft (0.021 m/m). Solids feed rates of 100 and 200 g/min (0.00167 and 0.00333 kg/sec) and pipe rotational speeds of 2, 5, and 8 rpm (0.033, 0.083, and 0.133 rps) were used. Table 2 summarizes the experimental conditions for these tests.

Since solids are mixed and redistributed several times during their movement through the vessel, these disturbances can be considered to be statistical in nature. Thus the mechanism for dispersion in analogous to molecular diffusion, and similar governing differential equations can be written. If these equations are put in dimensionless form, the

Table 2. Experimental conditions for the RTD tests (6-in.-diam pipe)

Run number	Feed rate		Drum rotational speed	
	g/min	kg/sec	rpm	rps
4	100	0.00167	2	0.033
5	100	0.00167	8	0.133
6	100	0.00167	5	0.083
7	200	0.00333	5	0.083
8	200	0.00333	8	0.133
9	200	0.00333	2	0.033

Drum slope = 0.25 in./ft.

dimensionless variable $\theta = \frac{t}{\bar{t}}$ appears, where

θ = reduced effective residence time,

t = time after step change, sec,

$\bar{t} = M/\dot{m}$ = mean residence time, sec,

M = total bed mass, kg,

$\dot{m}$ = solids mass flow rate, kg/sec.

The expected response to a step input in a system with dispersion is an S-shaped curve, the exact shape being determined by the system characteristics.

Figure 2 summarizes the data obtained in runs 4 through 9. The mass fraction of tracer from the vessel exit is plotted as a function of the reduced effective time, θ. All the data can be represented by this single plot since the amount of dispersion did not vary significantly with the operating variables. In this plot, the mass fraction range at $\theta = 1$ is above 0.5. This may be due to entrance or exit effects; material is dispersed inside the kiln but not in the feed or product. The results reported here compare favorably with those obtained in earlier work using a commercial unit. This replication of experiments and results provides a basis for the design of experiments to follow, namely, experiments with a larger-diameter unit. Residence time distribution studies will also be designed and carried out to determine the effects of feed size distribution and lifting flight configuration. This will provide design information as well as give insight into internal flow patterns.

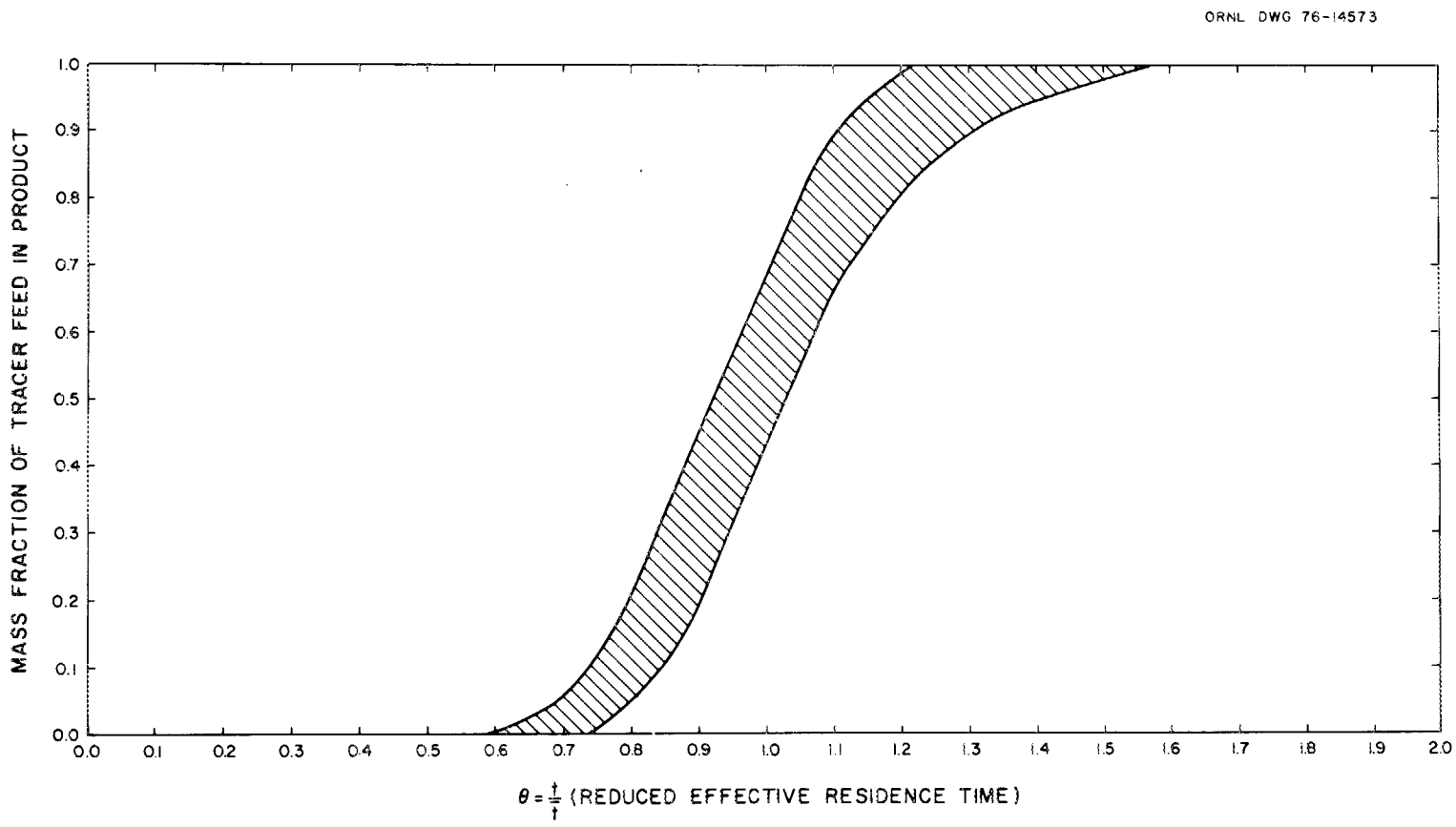

Fig. 2. Residence time distribution data obtained using a 6-in.-diam, 7.0-ft-long rotating pipe.

2.1.3 Component development

D. C. Hampson and M. E. Whatley (Chemical Technology Division, ORNL)

In pursuit of the procurement of a larger-scale rotary kiln voloxidizer for study and testing, a bid package of specifications and criteria for design and fabrication was prepared and issued to candidate suppliers. This unit will be sized to handle 1/2 metric ton of fuel per day and will be more flexible, both in heating capability and in instrumentation, than will be required in a production-type unit. The deadline for bid submission has been extended from mid-September to October 12, 1976.

The auxiliaries such as the feeding system and the off-gas treatment system are not part of the above purchase, but will be developed at ORNL. Criteria for these systems have been prepared, and design has been started.

2.2 Hot-Cell Studies

D. O. Campbell (Chemical Technology Division, ORNL)

An experimental program centered around hot-cell tests of fuel reprocessing operations was initiated in January 1976. A variety of LWR fuels will be used; however, most work to date has been done with fully irradiated PWR fuel cooled about 2 years. The work is supported by "cold" experiments with synthetic solutions similar in chemical composition to true process solutions.

The ORIGEN calculation was tailored to the Robinson reactor irradiation history, using the best data we could obtain, with the valuable assistance of A. G. Croff. These calculated results are in much better agreement with experimental data, especially plutonium isotopic content, than were earlier calculations.

Two fuel dissolutions were completed during this quarter (runs 5 and 6); experimental work on the four previous runs was also completed. Each complete experiment includes a study of most or all of the following operations: fuel dissolution; off-gas scrubbing with special attention to the behavior of ^{3}H, ^{14}C, and ^{129}I; clarification of the dissolver solution; rinsing of the dissolver, cladding (if any), and undissolver residues; solvent extraction of uranium and plutonium; evaporation of the raffinate to produce a waste concentrate; aging of process solutions to study solution stability; characterization of any solids formed; and waste partitioning studies, which are reported elsewhere.

Analytical results are essentially complete for the first five runs, but not the sixth. A major effort is presently directed toward data analysis and interpretation. In general, the tentative conclusions stated in the introduction to Sect. 2.2 of the previous quarterly report[6] have been reinforced or confirmed; none has been contradicted. In many cases, quantitative data are now available from more than a single experiment.

Dissolution of fully irradiated fuel under conditions approximating projected operations at AGNS is satisfactory except that a somewhat longer dissolution time will be necessary.

Approximately 0.2 to 0.3 wt % of the irradiated fuel is insoluble during dissolution in HNO_3. This residue is extremely radioactive due to the presence of fission product ruthenium; it may also contain up to a few tenths percent of the plutonium and the other actinides. Leaching the residue with nitric acid reduces the actinide content to a few thousandths

percent, although the bulk of the material remains insoluble. In full-scale reprocessing, this insoluble fraction will require attention because of its heat generation properties.

The fraction of ^{129}I remaining in the dissolver solution may be reduced to less than 1% of the amount present. Nitrogen oxides produced during dissolution remove greater than 90% of the iodine, and air sparging either during or following dissolution will transfer additional iodine to the off-gas.

Incomplete data for ^{14}C indicate that most of the carbon reports to the first caustic scrubber in the off-gas system. There is no evidence for organic carbon in the off-gas. The total amount of ^{14}C found is consistent with a nitrogen content in the fuel of about 10 ppm, which is reasonable.

The dissolver solution is probably stable to formation of the insoluble Zr-Mo compound for several days, provided the temperature is not too high or the acidity too low. This compound would carry a significant fraction of the plutonium if it precipitated prior to extraction.

Solids are more readily produced when the extraction raffinate is aged. Well-crystallized solids form slowly from 3 to 4 M HNO_3 raffinate, and x-ray diffraction shows them to have the same structure as the Zr-Mo compound prepared previously in cold work. The solids, which are highly enriched in ^{125}Sb, carry several percent of the plutonium present in the raffinate.

No significant problem has been encountered with regard to plutonium extractability. Batch extractions are carried out a few days after dissolution without valence adjustment. The distribution coefficient for plutonium did not decrease during extraction of at least 99.9% of the plutonium.

Evaporation of the extraction raffinate at 7 to 10 M HNO_3 resulted in the appearance of solids at a waste concentration of about 325 gal per metric ton of fuel, a significantly lower concentration than has been achieved with synthetic waste. The solids are not yet characterized. The concentrated waste supernate has been stable for more than one month.

2.2.1 Hot-cell dissolution

D. O. Campbell, S. R. Buxton, R. L. Beatty, and W. L. Pattison (Chemical Technology Division, ORNL)

Two additional experiments have been completed with fully irradiated (31,360 MWd/MTU*) fuel from the Carolina Power and Light H. B. Robinson II reactor, discharged on May 6, 1974. Run 5 was designed to test the effect of the use of recycle nitric acid for dissolution and of the time interval between dissolution and extraction on plutonium extractability. Run 6 was made primarily to determine more accurately the relative distribution of radioisotopes into cladding hulls.

In run 5, 364.9 g of unclad UO_2 fragments from the full burnup region (24.5 to 121.5 in.) of Rod O-14 of Assembly B05 was dissolved in HNO_3, much of which was recovered by distillation (waste evaporation) of the extraction raffinate from run 4. Some new concentrated HNO_3 was used to provide the total acid requirement. Dissolution proceeded normally, and there were no obvious effects from the use of recycle acid. The amount of insoluble residue after dissolution was consistent with previous experiments (Sect. 2.2.3).

This dissolution was made without an air sparge. A small fraction of the off-gas was lost when the evolution of nitrogen oxides exceeded the

---

* MTU = metric tons of uranium.

capacity of the off-gas scrubber for a short time because of a partial plugging of the first scrubber. Following completion of dissolution, as indicated by a cessation of bubbling in the dissolver, the dissolver solution was air sparged for 160 min at 0.4 solution volume of air per minute. Evolution of ^{129}I is discussed in Sect. 2.2.2.

A portion of the dissolver solutions was transferred to M. H. Lloyd for detailed solvent extraction studies as quickly as possible after dissolution. Extractions were initiated less than 24 hr after dissolution, compared with several days in all previous cases. Although the time between dissolution and extraction is not well-defined for an actual operation, it would likely vary between 1 and 3 days for AGNS. Results of the study are described in Sect. 2.2.4.

Most of the dissolver solution was batch extracted to the extent of about 99.8% of the uranium and plutonium, and the raffinate was evaporated at an HNO_3 concentration of 7 to 10 M in the still pot, to the rather high final concentration of about 60 gal/MTU processed. The results are described in Sect. 2.2.5.

The dissolution in run 6 was made with all the clad fuel of full burnup that we have obtained to date. We have several clad end-pieces such as were used in run 3, but the effective burnup for this material is uncertain. The fuel in run 6 consisted of 14 pieces ranging from 0.3 to 2 in. long, all from the region of burnup greater than 30,000 MWd/MTU of fuel rods H-10, P-4, and P-8 of Assembly B05.

The dissolution deviated seriously from reference conditions, primarily because the temperature was much higher and significant boiling occurred. A much greater volume of condensate was collected, with the result that

the dissolver solution was concentrated to a value above the solubility of uranyl nitrate at room temperature. Accordingly, large crystals of uranyl nitrate hexahydrate were recovered along with the dissolver residue during fuel clarification.

In spite of the departure from reference conditions, no problems were encountered which could not be dealt with readily in a processing plant. The dissolution was probably more complete than usual. Dilution of the dissolver solution to compensate for the loss due to distillation appeared to yield a normal solution.

Following dissolution, the cladding was removed, rinsed, weighed, and all except two pieces were dissolved in an $HF-HNO_3$ solution. A small amount of residue which did not dissolve in this solution was dissolved by Na_2CO_3 fusion. The quantity of various radioisotopes associated with cladding is being determined, but these results are not yet available. This is an important factor relative to hull monitoring for undissolved fuel.

Analysis of the cladding from run 3 did not yield definitive results because of uncertainty concerning the actual burnup, which varied along the length of the fuel by as much as a factor of 4. The data indicated that the cladding contained about 1 to 2% of the fission products, less than 0.01% of the transuranium elements, and less than 0.001% of the uranium. These quantities all produced when the product nuclei recoil following nuclear reaction, ejecting atoms from the outer fuel region into the cladding. Since fission fragments have a much greater recoil energy than transuranium elements, more are ejected. The important point is that

monitoring of a gamma-emitting fission product would indicate a much higher holdup with the cladding than the actual amount of the elements of interest, uranium and plutonium.

2.2.2 Radioactivity in off-gas

D. O. Campbell, S. R. Buxton, R. L. Beatty, and W. L. Pattison (Chemical Technology Division, ORNL)

Additional data have been received for ^{129}I distribution during fuel dissolution (see Table 3). The results for runs 2, 4, 5, and 6, which were made with full-burnup Robinson reactor fuel, should be fairly similar. The ORIGEN calculation has been made for the irradiation history of this reactor. It is clear that the overall material balance is reasonably good in each case except run 3. The calculated ^{129}I values for runs 1 and 3 are less certain.

Table 3. ^{129}I distribution during fuel dissolution

Run number	^{129}I found		Percent of total found in:			
	g/MTU	% of ORIGEN value	Dissolver	Condensate	Scrub 1	Scrub 2
1	118	82	0.52	0.14	99.3	0.08
2	157	84	0.97	1.08	97.4	0.57
3	45	41	0.50	0.90	98.3	0.30
4	Not complete					
5	169	90	0.22	0.21	99.4	0.18
6	141	75	0.93	1.12	96.4	1.53

In all cases, less than 1% of the ^{129}I found was in the final dissolver solution. The fraction found in the condensate in this work would probably

be largely transported to the scrubbers in plant equipment because, in our equipment, the off-gas flow bypassed the condensate and thus could not strip iodine from it.

In run 4 (with UO_2 fragments) and run 5 (with clad fuel and recycle acid), there was no air sparge during dissolution; however, the solution was sparged for several hours after dissolution. The data for ^{129}I removal are summarized in Table 4. Although significantly more iodine remained in the dissolver solution after run 5, the air sparge reduced the iodine to a few tenths of 1% in both runs.

Table 4. Effect of duration of air sparge on ^{129}I content of dissolver solution

Run 4		Run 5	
Time (min)	% ^{129}I[a]	Time (min)	% ^{129}I[a]
0	1.52 ± 0.13	0	5.73 ± 0.13
70	0.42 ± 0.09	85	1.25 ± 0.54
140	0.24 ± 0.03	160	0.29 ± 0.09
200	0.17 ± 0.02		

[a]Percent of ^{129}I remaining in dissolver solutions, relative to total amount calculated by ORIGEN.

These experiments show that iodine was effectively stripped from the dissolver solution, most of it by the nitrogen oxides evolved in the dissolution reaction. Sparging with air further reduced the iodine content, with no indication of any leveling off at 0.2%. The use of recycle acid that could contain some organic material had no effect on the final iodine content. Volatile organic iodides would not be trapped by caustic scrubbing

but would be decomposed by the CuO bed and trapped in the second scrubber. Since the second scrubber trapped very little iodine, the quantity of volatile organic iodide present (if any) must be minimal.

Data for ^{14}C for the first four runs are summarized in Table 5. The major source of ^{14}C is the n,p reaction with nitrogen impurity in the fuel. The tabulation reports the nitrogen content of the fuel, back-calculated from the amount of ^{14}C found (neglecting the n,α reaction on ^{17}O).

Table 5. ^{14}C distribution during fuel dissolution

Run number	^{14}C found (Ci/MTU)	Nitrogen content (ppm, calc.)	Percent of total found in:			
			Dissolver	Condensate	Scrub 1	Scrub 2
1	0.14	7.7	[a]	[a]	99.5	0.5
2	0.27	10.4	[a]	0.44	97.5	2.1
3	0.15	10.3	[a]	0.65	97.5	1.85
4	0.24	9.3	[a]	0.41	58.7	40.9

[a]Analytical results are not complete.

Information regarding the nitrogen content of the Robinson fuel (runs 2, 3, and 4) was requested from workers at Westinghouse, who reported that analyses of several different batches of UO_2 pellets from this fuel gave nitrogen values of less than 10 ppm, the limit of detection. We plan to attempt to measure the nitrogen content presently in the irradiated fuel used for these experiments in order to define the value more accurately. Only a very small fraction of the nitrogen was transmuted to other elements; therefore, values determined in this measurement should correspond closely to the initial nitrogen content of the Robinson fuel (excluding elemental nitrogen such as that in air).

We have obtained conflicting information regarding nitrogen in the gas that occupies the fuel rod void volume. A verbal report from Westinghouse indicated that the rods contained air before welding, but other information suggests they were filled with helium. Postirradiation analysis of gas removed from other rods of this same assembly showed the rods were predominantly filled with helium, but some nitrogen was present. However, the zirconium cladding probably would have reacted with both oxygen and nitrogen during reactor operation, so they might not be found after irradiation.

If the fuel rods were initially filled with air at 1 atm pressure, nitrogen in this air would contribute about 10 ppm relative to uranium; and this agrees with the nitrogen content indicated by ^{14}C analysis. Nitrogen impurity in the UO_2 provides an additional source of ^{14}C.

The conclusion is that the amount of ^{14}C found is in reasonable agreement with the calculated value for this fuel; part of it probably results from nitrogen in air sealed in the fuel rods. Carbon is effectively trapped in the caustic scrubbers and is presumably released during dissolution as CO_2. Experimental evidence indicates that CO or organic carbon compounds are formed in extremely small amounts, if at all.

Work is continuing to develop a method to analyze for ^{14}C, ^{129}I, and ^{3}H, which might be present in the dissolver solution as nonvolatile (organic) compounds. Laboratory tests indicate that wet oxidation with perchloric acid under reflux, followed by CuO oxidation of an air sweep and finally caustic scrubbing, will recover ^{14}C from both aromatic and aliphatic hydrocarbons and organic compounds such as acetic acid, benzoic acid, and nitrobenzoic acid. This method will be used with the dissolver solution as a final test for ^{14}C and ^{129}I that may not have been found so far.

No additional data are available for tritium.

2.2.3 Insoluble dissolution residue

D. O. Campbell, S. R. Buxton, R. L. Beatty, and W. L. Pattison (Chemical Technology Division, ORNL)

The insoluble residue from runs 5 and 6 constituted 0.23 and 0.44%, respectively, of the weight of UO_2. Dissolution conditions in run 6 were unusually severe, and a smaller fraction of residue was expected. However, the larger amount may result from oxide film removed from the cladding. With reasonably complete dissolution, the residue typically comprises between 0.2 and 0.3% of the weight of UO_2.

The reproducibility of dissolver compositions is illustrated by the data of Table 6, which summarizes the total quantities of a number of radioisotopes found in the dissolver solutions from runs 2, 4, and 5. All of these runs were made with fully irradiated Robinson fuel; however, two different rods were used. For reference, the corresponding quantities calculated by the ORIGEN code are given.

Agreement with the ORIGEN calculations is rather good in many cases. However, significant discrepancies occur for the heavier actinides (the analytical results for americium are subject to error because of interference from ^{238}Pu, but the values for the other actinides should be valid), for ruthenium (much of which does not dissolve), and for those isotopes resulting from a neutron capture reaction following fission (such as ^{134}Cs and ^{154}Eu). There is also an apparent systematic discrepancy in the experimental results since the values for runs 4 and 5 are about 5 and 9% higher, respectively, than those for run 2.

Table 6. Calculated and observed radioisotope concentrations in dissolver solutions (March 16, 1976)

Isotope	Conc. calculated by ORIGEN code		Experimentally determined conc. (Ci/MTU)		
	dis sec^{-1} ml^{-1} [a]	Ci/MTU	Run 2	Run 4	Run 5
^{238}Pu	2.6×10^{7}	2.11×10^{3}	2.41×10^{3}	2.80×10^{3}	2.84×10^{3}
$^{239,240}Pu$	1.04×10^{7}	8.42×10^{2}	8.00×10^{2}	9.73×10^{2}	8.49×10^{2}
^{241}Am	6.99×10^{6}	5.67×10^{2}	3.41×10^{2}	1.54×10^{2}	3.04×10^{2}
^{244}Cm	5.85×10^{7}	4.74×10^{3}	1.97×10^{3}	2.09×10^{3}	2.22×10^{3}
^{242}Cm	1.98×10^{7}	1.60×10^{3}	2.67×10^{3}	2.38×10^{3}	2.49×10^{3}
^{106}Ru	1.90×10^{9}	1.54×10^{5}	5.57×10^{4}	8.22×10^{4}	8.14×10^{4}
^{134}Cs	1.40×10^{9}	1.14×10^{5}	6.58×10^{4}	6.9×10^{4}	7.17×10^{4}
^{137}Cs	1.23×10^{9}	9.99×10^{4}	8.52×10^{4}	9.05×10^{4}	9.48×10^{4}
^{144}Ce	2.33×10^{9}	1.89×10^{5}	1.75×10^{5}	1.83×10^{5}	1.86×10^{5}
^{125}Sb	8.04×10^{7}	6.52×10^{3}	$\leq 3.46 \times 10^{3}$	$\leq 5.02 \times 10^{3}$	$\leq 3.16 \times 10^{3}$
^{154}Eu	1.70×10^{8}	1.38×10^{4}	$\leq 3.62 \times 10^{3}$	N.A.	4.04×10^{3}
^{90}Sr	8.10×10^{8}	6.57×10^{4}	5.31×10^{4}	N.A.	6.81×10^{4}
^{95}Zr	7.91×10^{6}	6.41×10^{2}	$\leq 2.05 \times 10^{3}$	N.A.	N.A.
^{3}H	5.36×10^{6}	4.35×10^{2}	2.57×10^{2}	3.08×10^{2}	N.A.
^{14}C [b]	6.59×10^{3}	5.34×10^{-1}	N.A.	N.A.	N.A.
^{129}I	4.03×10^{2}	3.27×10^{-2}	2.34×10^{-4}	5.22×10^{-5}	4.98×10^{-5}

[a] Based on 1.4 M $UO_2(NO_3)_2$ = 333 g of uranium per liter.

[b] Assuming that the UO_2 has a nitrogen content of 20 ppm.

N.A. = not available.

The distribution of radioisotopes between the dissolver solution and the solids residue is summarized in Tables 7 and 8 for runs 2 and 4, respectively. The column headed "Washes" is primarily a measure of the fraction of the dissolver solution left in the dissolver after transfer plus the fraction associated with centrifuged solids. The column headed "Solids leach" gives the fraction of various isotopes that dissolved in 3 M and 6 M HNO_3 at 90°C for run 2 and in 12 M HCl for run 4; HCl dissolves nearly all the residue. The last column is the fraction remaining in the solids after leaching.

Of these isotopes, only ruthenium is present at significant levels in the solids residue; half or more of the ruthenium may remain undissolved in the HNO_3. Ruthenium is a significant heat source; thus the separation and disposition of this residue must take heat generation into account. A 5-ton/day plant will produce approximately 10 to 15 kg per day of these solids, with a heat output of 3 to 5 kW.

The residue obviously contains other elements besides ruthenium, but data for the nonradioactive elements are still being evaluated. Molybdenum is an important constituent, and technetium, rhodium, and palladium may also be present, along with tramp material related to dust and glass. The composition of the residue will not be reported until more dependable analytical results are derived.

We are using spark-source mass spectrometry (SSMS) for the general analysis of stable isotopes (as well as radioactive isotopes present in reasonable amounts). Considerable work is being done to improve the accuracy of this method. Recently, the sample preparation procedure was

Table 7. Distribution of radioisotopes during dissolution in run 2 (212 g of uranium)

Isotope	Quantity found (Ci/MTU)	Calc. by ORIGEN code (% of found)	Percent of total found in fraction			
			Dissolver solution	Washes	Solids leach[a]	Leached solids
^{238}Pu	2.41×10^3	87	99.96	0.02	0.011	0.0004
$^{239,240}Pu$	800	105	99.96	0.02	0.010	0.0003
^{241}Am	341	166	100	-	-	-
^{244}Cm	1.97×10^3	241	99.97	0.02	0.006	0.0013
^{242}Cm	2.67×10^3	60	99.97	0.02	0.009	0.0017
^{106}Ru	12.2×10^4	127	47.53	0.41	8.5	43.56
^{134}Cs	6.58×10^4	173	99.96	0.02	0.007	0.010
^{137}Cs	8.52×10^4	117	99.96	0.02	0.008	0.011
^{144}Ce	17.5×10^4	108	99.95	0.02	0.026	0.024

[a]Solids leached with 3 M and 6 M HNO_3.

Table 8. Distribution of radioisotopes during dissolution in run 4 (314 g of uranium)

Isotope	Found (Ci/MTU)	ORIGEN (% of found)	Percent of total found in fraction			
			Dissolver solution	Washes	Solids leach[a]	Leached solids
^{238}Pu	28.1×10^3	75	99.66	0.31	0.015	0.019
$^{239,240}Pu$	977	86	99.97	0.28	0.009	0.023
^{241}Am	155	365	99.29	0.58	0.113	0.017
^{244}Cm	2.10×10^3	226	99.60	0.37	0.008	0.026
^{242}Cm	2.27×10^3	71	99.60	0.38	0.007	0.016
^{106}Ru	13.4×10^4	115	61.17	0.22	37.02	1.59
^{134}Cs	6.93×10^4	164	99.62	0.31	0.066	0.002
^{137}Cs	9.08×10^4	110	99.63	0.33	0.042	0.003
^{144}Ce	18.4×10^4	103	99.58	0.31	0.100	0.007

[a]Solids leached with 12 M HCl.

modified to incorporate additional standard isotopic spikes, which will be added in two different groups. In addition, radioisotope analyses are being made to provide a check on the SSMS method for several elements.

More meaningful comparisons of calculated with experimental data, relative to material balances, are provided by mass analyses because the experimental determinations are much less subject to error. Mass analysis data for uranium, plutonium, americium, and curium* recovered from run 2 are reported in Table 9. These measured values for uranium and plutonium are in reasonable agreement with the results of ORIGEN calculations. The americium values are satisfactory except for a large error in the very low yield mass 242. Agreement is rather poor for curium. Since the discrepancies become larger for the heavier actinides, it appears that some refinement may be necessary for the nuclear data used in the ORIGEN code for actinide production.

2.2.4 Plutonium extraction into 30% TBP**

M. H. Lloyd (Chemical Technology Division, ORNL)

In connection with studies to investigate the nature and behavior of "inextractable" plutonium in high-level fuel reprocessing and waste streams, plutonium extraction behavior was evaluated with radioactive feeds prepared

---

*The isolation of americium and curium was carried out by the staff of the Transuranium Reprocessing Plant (TRU).

**Studies carried out as part of a program on Waste Stream Processing Studies funded by the Molecular Sciences Branch of the Division of Physical Research, ERDA.

Table 9. Mass analysis of actinides from run 2[a]

H. B. Robinson Fuel
Burnup: 31,364 MWd/MTU
Reactor shutdown: May 6, 1974
Separation: March 16, 1976

Actinide	Found	ORIGEN	Actinide	Found	ORIGEN
^{234}U	0.014	0.013	^{241}Am	62.4	65.95
^{235}U	0.653	0.615	^{242}Am	0.312	0.0002
^{236}U	0.347	0.352	^{243}Am	37.29	34.02
^{237}U	[b]	3E-9			
^{238}U	98.99	99.02	^{242}Cm	3.28	1.00
			^{243}Cm	1.21	0.14
^{238}Pu	1.56	1.32	^{244}Cm	90.66	97.57
^{239}Pu	55.79	56.72	^{245}Cm	4.43	1.14
^{240}Pu	24.91	23.87	^{246}Cm	0.453	0.152
^{241}Pu	12.29	12.73	^{247}Cm	0.004	0.002
^{242}Pu	5.45	5.36	^{248}Cm	0.001	0.0002

[a]Atom % of each as of March 16, 1976.

[b]Not detected.

from highly irradiated UO_2. In each experiment, the UO_2 dissolver solution, which had a HNO_3 concentration of approximately 3 M, was batch-contacted with equal volumes of 30% TBP--dodecane. Seven consecutive extraction stages were used.

In previously reported extraction experiments, the feed solutions were aged 2 to 3 weeks prior to extraction, and the plutonium valence in each was found to be quantitatively in the tetravalent state. In recent work, a UO_2 feed solution extracted 20 hr after dissolution was found to contain about 20% Pu(VI).

Except for a somewhat lower distribution coefficient due to the Pu(VI) content, the plutonium extraction behavior for this material was quite comparable to that observed in previous runs, in which the feeds contained only Pu(IV). The extraction data are compared with results from a Pu(IV) run in Fig. 3, which shows the plutonium concentration (in counts min^{-1} ml^{-1}) remaining in the aqueous raffinate after each stage. These data indicate that, even though Pu(VI) is not extracted as effectively, greater than 99.99% of the plutonium was extracted in seven stages.

The plutonium concentrations shown for the last two stages of the Pu(VI) run were subject to a large correction factor due to the growth of ^{238}Pu from ^{242}Cm decay, which occurred after the extractions were made but before the solutions were analyzed. The actual values could therefore be somewhat higher or lower than the concentrations shown. Efforts will be made to minimize this effect in future experiments.

The plutonium behavior in this experiment suggests that the initial UO_2 dissolver solution contains substantial concentrations of Pu(VI), which subsequently reduces to Pu(IV) in the highly radioactive feed

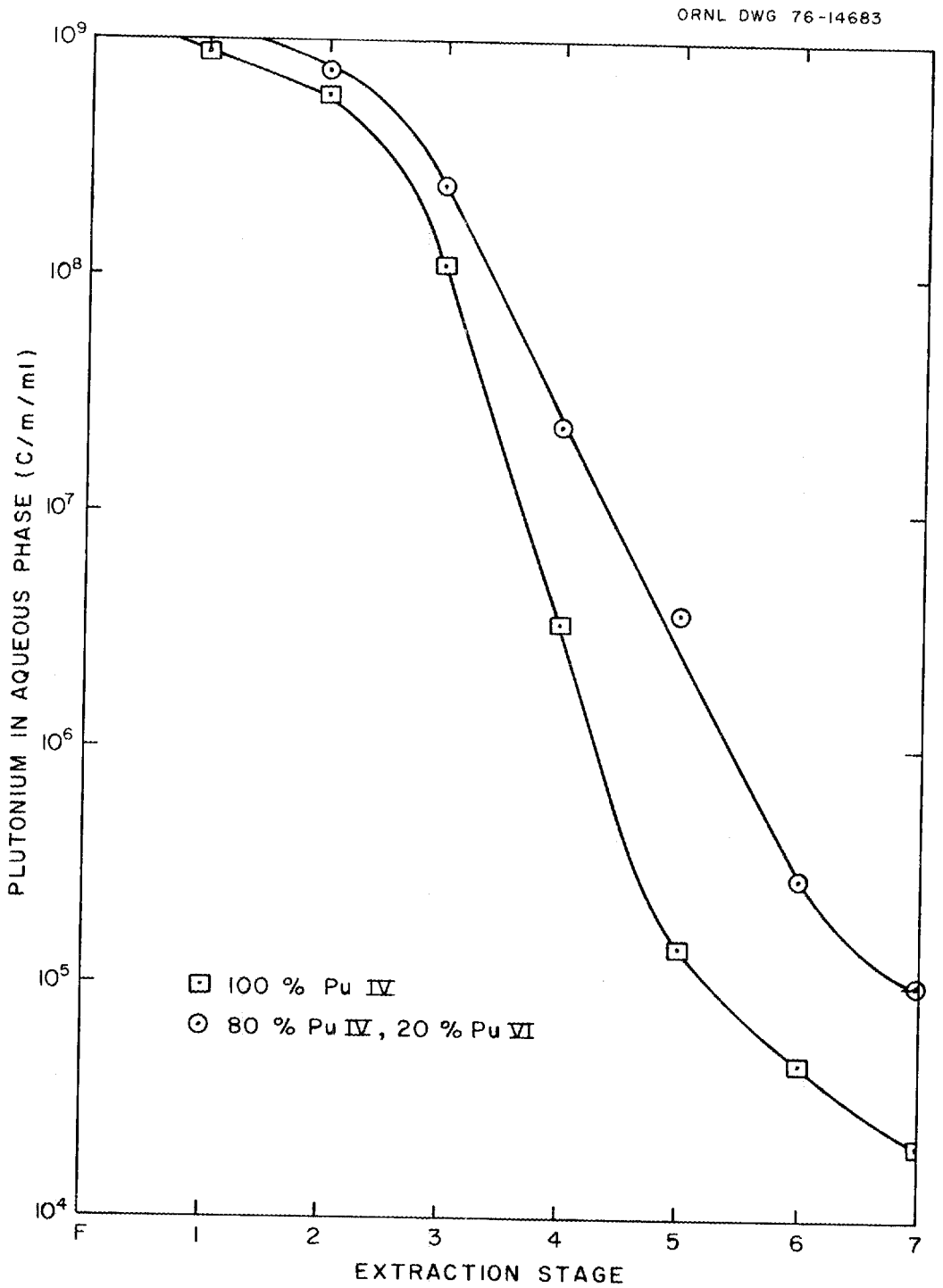

Fig. 3. Plutonium extraction behavior from feed prepared by dissolution of irradiated UO_2. Feed adjusted to 3 M HNO_3 was contacted with equal volumes of 30% TBP--dodecane. UO_2 fuel: Assembly B05, Carolina Power and Light H. B. Robinson reactor fuel irradiated to 31,360 MWd/metric ton.

solution. An experiment was therefore performed to determine the approximate rate at which Pu(VI) is reduced in UO_2 dissolver solution. More than 95% of the plutonium in a 3 M HNO_3 feed solution was oxidized to Pu(VI) by heating the solution at the boiling point (~108°C) for several days. The solution was then cooled to 40°C, and the rate of plutonium reduction was determined. The percent of tetravalent plutonium after 1, 2, and 3 days of aging was found to be 42, 90, and 100, respectively.

2.2.5 Solution stability

D. O. Campbell, S. R. Buxton, R. L. Beatty, and W. L. Pattison (Chemical Technology Division, ORNL)

No additional results have been obtained from solution stability tests, although several aging experiments are still in progress. A different sort of instability that has been noted in the dissolver solution is receiving increased attention.

We have observed that a small quantity of black solids, similar in appearance to the original dissolver residue, appears in the clarified dissolver solution after a few days. The dissolver solutions from runs 5 and 6 were centrifuged several times at intervals of a few days, and additional black solids were recovered in every case. The quantity of this material is small; preliminary measurement indicates it is in the range of 50 mg per day per kg of fuel (±50%).

Samples of these solids have been submitted for scanning electron microscope (SEM) and microprobe analyses, and the solids have been dissolved and submitted for radiochemical and SSMS analyses. No results have been obtained to date.

Although the quantity of solids is very small, their formation appears to be real. Initially, they were believed to result from incomplete solids recovery during centrifugation, but the constant production with repeated centrifugation contradicts that suggestion. Since any such solids will almost certainly collect at the solvent interface and compound the interfacial crud problem, feed clarification immediately prior to solvent extraction may be a more important consideration than previously indicated.

Waste concentration. A portion of the extraction raffinate from run 5 was concentrated by distillation in a manner similar to that used in the two previous waste evaporation experiments. General behavior was similar to that observed in the earlier tests, with solids first appearing at a waste concentration of about 300 to 350 gal/MTU and increasing in amount as evaporation proceeded. The evaporation was continued to a final concentration of about 60 gal/MTU. The total amount of solids recovered was 1.8 g per kg of uranium processed, and an appreciable fraction may have been lost.

We are now receiving analytical data relating to the solids produced during waste evaporation; however, it has not yet been correlated. Preliminary observation of the data indicates that substantial amounts of Ba, Sr, Mo, and Cs are present, along with tramp material such as Ca, Mg, Si, Al, and Fe.

Efforts have continued to determine the rate of acid loss in air-sparged solutions, such as would occur during waste storage. This has proved to be more difficult than expected because of analytical problems with the extremely radioactive waste concentrates and experimental difficulties relative to the small volume of solution and possible evaporation.

Refinement in the acid titration procedure has resulted in improved precision, generally ±0.1 M, and has eliminated the occasional large errors observed previously. The titration problems appear to be related to some aspect of radiation damage.

The extraction raffinate from run 5 (about 800 gal/MTU) was air-sparged for 10 days with inconclusive results. The acidity appeared to decrease slightly, but any change was of the same magnitude as the analytical precision.

The clarified waste from run 4 (97 gal/MTU) was air-sparged at the rate of about 3 to 5 cc/min for 12 days, and eight samples withdrawn over this time period indicate an acid loss of about 0.03 mole per liter per day. This is not a clearly significant change; on the other hand, there may have been a volume decrease due to evaporation, in which case the acid loss could have been much greater.

The waste from run 5 (about 60 gal/MTU) was similarly air-sparged over a 14-day period, and the decrease in acid concentration appeared to be appreciably greater (i.e., roughly 0.1 mole per liter per day). In this experiment, the volume probably decreased more than could be accounted for by sampling. This could result from evaporation enhanced by a temperature rise of a few degrees due to the high concentration of radioactivity. The change in volume will be calculated when radioisotope analyses are obtained, and at that time the acid loss can be determined more accurately. This experiment with the highest concentration of waste is the only one that has resulted unambiguously in an acid loss.

A significant observation is that ruthenium is not volatilized to a large extent during these waste evaporation experiments. The nitric acid

concentration is in the vicinity of 9 M throughout the evaporation, and ruthenium would be expected to volatilize as RuO_4 to a major extent. In fact, it does volatilize in this manner when synthetic waste solutions are carried through an identical process, yielding large deposits of RuO_2 in the condenser as well as ruthenium in the condensate. No deposition of RuO_2 has occurred during the evaporation of actual waste solution, and the condensate typically contains about 0.2% of the total ruthenium present. This amount of ruthenium, although a factor of 5 to 10 higher than other fission products, is still remarkably low. It appears that a quite stable complex is formed between ruthenium and some radiolysis product that inhibits formation of RuO_4.

2.2.6 Characterization methods

D. O. Campbell (Chemical Technology Division, ORNL)

Work continues to improve the methods we have been using throughout, especially SSMS and x-ray fluorescence, to yield more accurate and meaningful data. The SSMS sample preparation procedure was changed, as described in Sect. 2.2.3. Equipment was assembled and tested to recover any organic carbon, hydrogen, or iodine which may be present in solutions such as dissolver solution (see Sect. 2.2.2).

A different approach is being tested for SEM and x-ray fluorescence sample preparation in an attempt to avoid the interferences that are obscuring the desired data. Interferences arise largely from copper and zinc in the brass sample mount, gold used to coat the sample, and lead from an undetermined source. Recently, several samples have been mounted on polished beryllium metal, and they will be coated with vapor-deposited carbon; this should give no interferences.

These specimens will also be examined for x-ray fluorescence by using a crystal wavelength dispersion x-ray detector instead of a silicon dispersion energy detector. This provides the possibility of shielding the detector from direct radiation from the sample, which cannot be done with the silicon detector. Such direct radiation has prevented x-ray fluorescence measurements from being made on about half the samples analyzed. The disadvantage of the new technique is that the measurement is much more time-consuming.

2.3 Building 4507 Hot-Cell Operations

J. H. Goode, R. G. Stacy, V. C. A. Vaughen, E. C. Hendren, and G. K. Ford
(Chemical Technology Division, ORNL)

2.3.1 Development of in-cell equipment

Testing of in-cell equipment was delayed in favor of using all personnel for decommissioning the Curium Recovery Facility (CRF). All of the equipment, however, was put in operating condition by the ORNL shops and is ready for further cold-testing as manpower becomes available.

2.3.2 Decommissioning the CRF

Ninety-five individual entries in air-line suits were made into the curium-contaminated CRF during the past quarter. The 2-ton, 13 x 3 x 9 ft tall Equipment Maintenance Glove Box, located above Cells 3 and 4 in Bldg. 4507, was separated from the floor, sealed, crated, and sent to storage in the ORNL Solid Waste Storage Facility.

Sandblasting was used to remove curium-contaminated paint from cell access holes and the concrete walls of the hot cells in the CRF. On completion of the sandblasting, the sand was bagged-out of the cells, and the surfaces were successively cleaned with a vacuum cleaner and washed

with detergent-water mixtures. Subsequent Health Physics surveys indicated a few hot spots that required additional cleaning, but the cells were generally at sufficiently low-contamination levels to permit preparations for resurfacing and repainting. These included removal and patching of unnecessary glove ports and windows from the sheetmetal alpha barrier in the rear of each cell, cutting and beveling piping for subsequent welding, masking pipe fittings for protection from paint, etc. Anchor-bolt holes were filled and the sandblasted concrete walls of Cell 3 plastered with stucco. Two coats of white epoxy paint were sprayed onto each cell and their access ports. After removal of the "vestibule" and "tent" used as contamination-control zones for personnel working in the cells, installation of fixed equipment in the cells will begin. These include plenums for cell ventilation exhaust filters, floor pans, work surfaces, etc. (Sect. 2.3.3).

2.3.3 Miscellaneous

The Garden Carrier No. 2 (AEC-OR-USA 6088/BLF) cask was returned from Battelle-Columbus Laboratory with the second shipment of irradiated UO_2 from the Carolina Power and Light H. B. Robinson II reactor. A portion of this second shipment was repackaged for another group at ORNL (Sect. 2.2), and a portion of the first shipment was packaged and sent to the Savannah River Laboratory in the Garden Carrier No. 2 along with an empty cask (D-38, AEC-OR-USA 5787/BLF) to pick up recycled SRP solvent for laboratory tests. The Garden Carrier was then sent to the Aerojet Nuclear Company, at Idaho National Engineering Laboratory (INEL), to pick up three complete rods from the H. B. Robinson reactor assembly B05.

Figure 4 shows the assembled working surface and fuel storage array ready for installation in Cell 3, Bldg. 4507, where shearing and voloxidation head-end studies will be performed. The ORNL Criticality Committee has approved the storage of 1.6 kg of ^{235}U + $^{239-241}Pu$ in the seven 7-in.-diam wells and sixteen 1-in.-diam wells. Lead-filled covers provide shadow-shielding overhead. Figure 5 shows the all-bolted construction of the support structure, the removable storage wells, and the cell exhaust plenum and a drop-in HEPA filter.

Figure 6 shows the intercell (Cell 2-3) transfer port with the doors closed and the sliding tray centered. Figure 7 shows one of the folding doors open and the trays projecting into a "cell."

Fabrication is in progress on floor pans for Cell 4 and a new sample chute for Cell 3. Design of a replacement Equipment Maintenance Glove Box and access hole shielding plugs is under way. Modification of a cask pedestal to place above the Cell 3 sample chute is in progress.

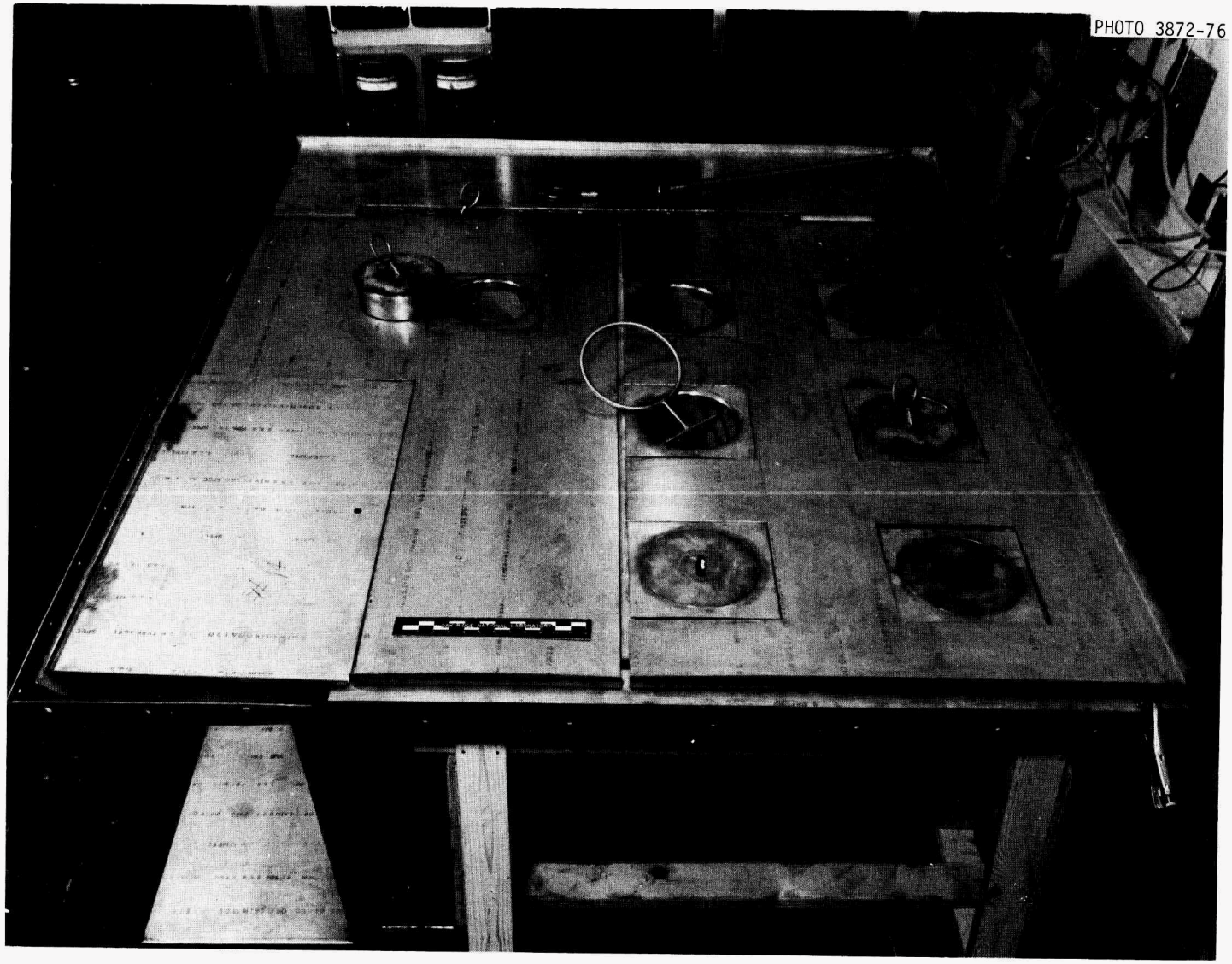

Fig. 4. Work tray and fuel storage wells for voloxidation cell.

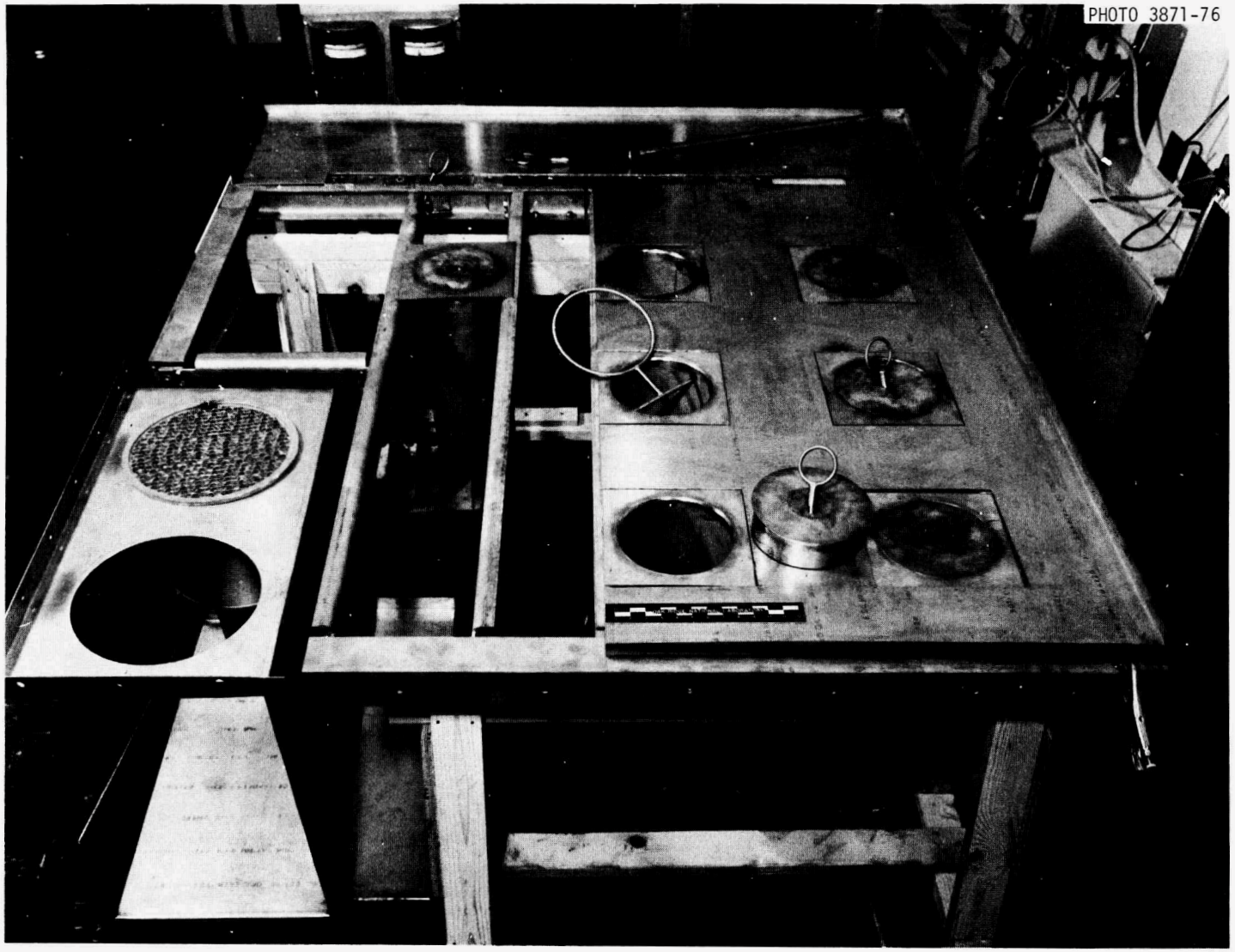

Fig. 5. Partially assembled work tray and fuel storage wells, showing bolted construction and cell exhaust plenum and HEPA filter.

PHOTO 3873-76

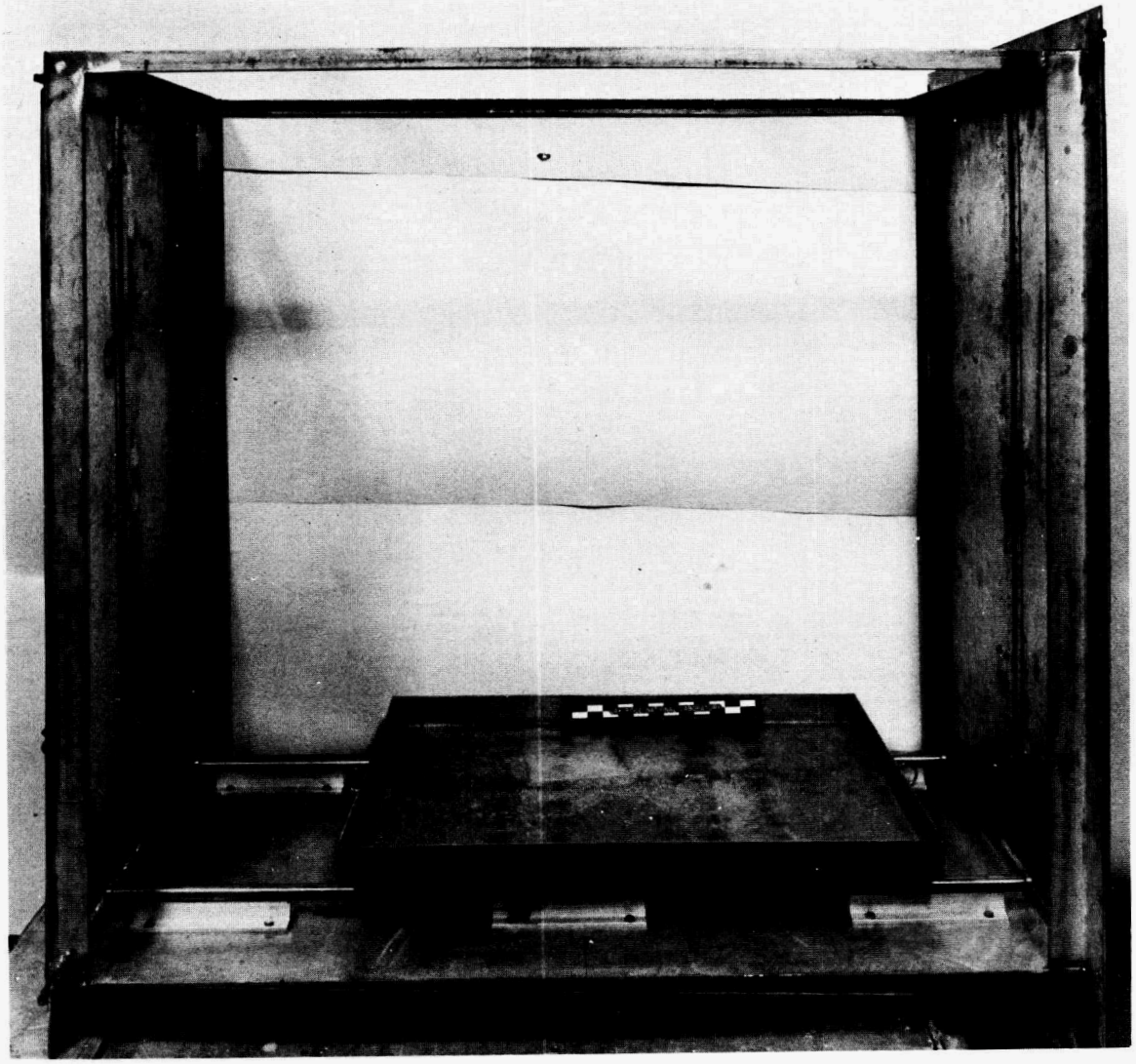

Fig. 6. Intercell transfer port.

PHOTO 3869-76

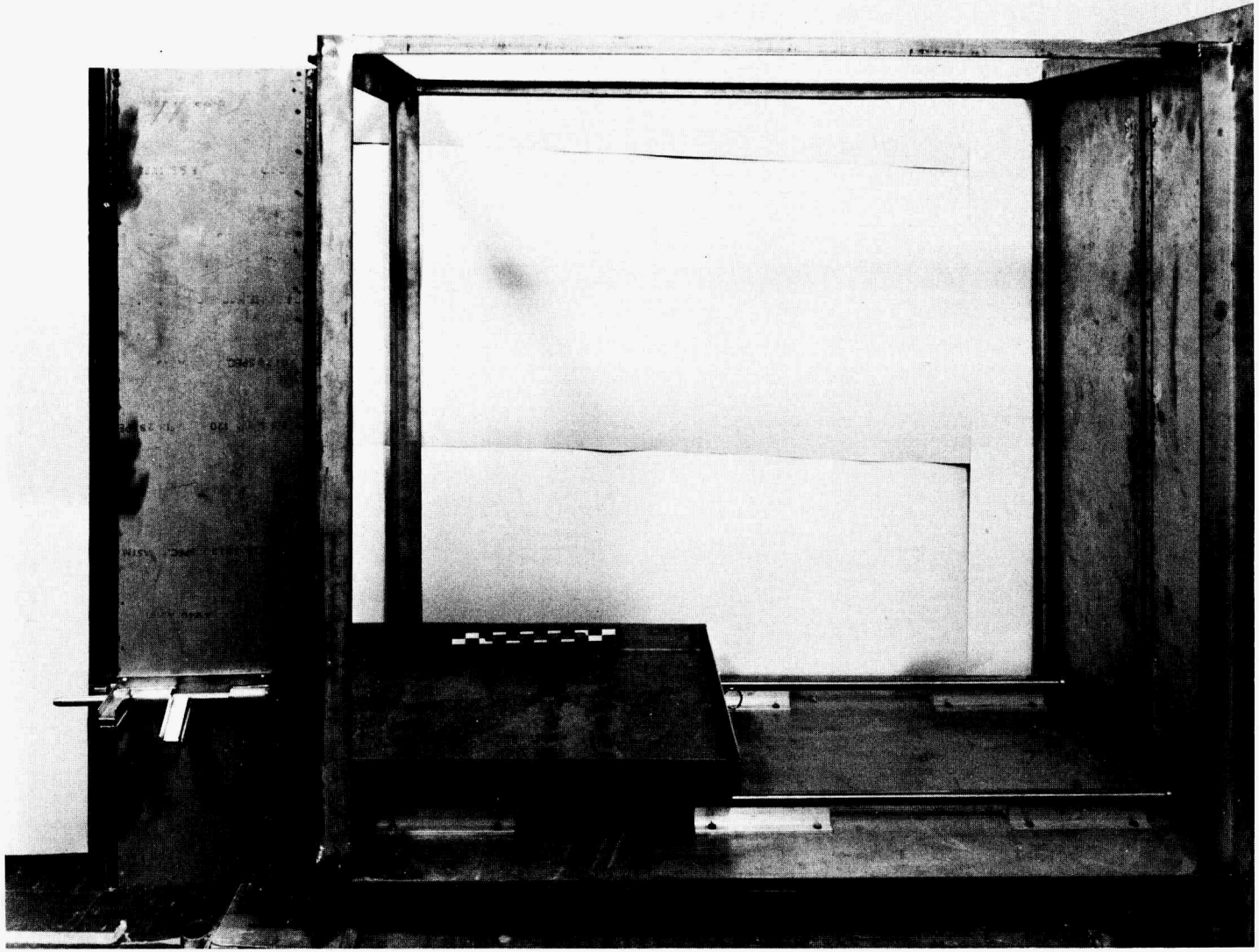

Fig. 7. Intercell transfer port with manipulator-operated door in open position.

3. PUREX PROCESS STUDIES (SOLVENT EXTRACTION)

B. L. Vondra (Chemical Technology Division, ORNL)

This program involves the integration of laboratory development studies, flowsheet tests employing synthetic solutions, and confirmatory investigations in a hot-cell system using irradiated LWR fuels.

3.1 Laboratory Studies

J. C. Mailen (Chemical Technology Division, ORNL)

3.1.1 Solvent cleanup

O. K. Tallent and Karen Williams (Chemical Technology Division, ORNL)

The solvent from the Purex process is presently treated with Na_2CO_3 and NaOH to remove impurities before it is reused. However, the lack of complete effectiveness of such caustic wash methods, along with attendant reagent recycle problems, has led us to investigate alternative solvent cleanup methods.

The objectives of this work are to evaluate, on a laboratory scale, a number of new (or partially new) methods for purifying recycle Purex solvents and to test the most promising of these methods on solvents from irradiated fuel extraction experiments. Ultimately, we expect to develop improved purification methods that are compatible with LWR and LMFBR fuel reprocessing flowsheets and meet criteria which results in: (1) production of a recycle solvent that is at least as effective as new solvent; (2) process steps that can be incorporated into the Purex flowsheet with no added foreign substance [NaOH, Na_2CO_3, etc.) recycle problems; (3) recovery of plutonium and other alpha-active actinides from the solvent

in easily accountable and processable form; and (4) isolation of impurities and fission products from the solvent in small volumes in easily processable forms.

Solid adsorbent tests. The use of solid adsorbents for removing impurities shows new promise of success, based on recent experimental evidence. Inorganic, organic, inert base, coated base, cation, and anion adsorbents and combinations thereof are being investigated. New loading and eluting techniques are being investigated along with new methods for reconstituting the solid adsorbents.

Experimental data have been obtained from tests using macroreticular resins as the solid adsorbent and dibutyl phosphate (DBP) and plutonium as solvent impurities. In each of the adsorption tests, 1.00 ± 0.01 g of moist resin was equilibrated with 10 ml of solvent at 25°C for 1.0 or 24.0 hr. The composition of the solvent was 30% TBP--0.00011 M DBP--0.00038 M Pu(IV)--0.03 to 0.73 M HNO_3 in dodecane. For the desorption tests, plutonium was adsorbed on 1 g of resin as described above, after which the effluent solvent was drained from the resin and the plutonium was desorbed by equilibrating the resin with 10 ml of 30% TBP--~0.70 M HNO_3 in dodecane for 1 hr at 25°C. Solvent samples were analyzed for plutonium using gross alpha and alpha pulse-height techniques. Effluent samples were not analyzed directly for DBP concentration; however, the plutonium retention power that can be used in these samples to approximately estimate DBP concentration was determined for three of the effluent samples. The test for plutonium retention consisted of adding 0.0038 millimole of Pu(IV) to 10 ml of effluent solvent, stripping or washing the solvent with three 10-ml volumes of 0.01 M HNO_3, and determining the plutonium concentration

retained in the solvent. Three of the adsorbent materials used in these tests, MP-1, MP-50, and SM-2, were Bio-Rad resins. The other two, A-15 and A-26, were Rohm and Haas resins. The MP-1, which is a strongly basic anion resin initially in the Cl^- form, was converted to the OH^- form by caustic and water washes before it was used in the adsorption tests.

The test results are shown in Table 10. The distribution coefficients listed in the table were calculated by dividing the concentration of plutonium adsorbed per gram of resin by the effluent plutonium concentration per milliliter. Plutonium adsorbed well from solvents with low acid concentrations on either MP-50 (cation), MP-1 (strongly basic anion), or A-26 (weakly basic anion) resin. The respective 1.0-hr distribution coefficients for these three resins were 1.9×10^3, 1.7×10^4, and 6.7×10^3, with the concentrations of plutonium retained in effluents being on the order of 1×10^{-7} M. The plutonium concentrations in these effluent samples were a factor of 1000 less than the 1×10^{-4} M plutonium retained in a sample of solvent feed which was washed three times with equal volumes of 0.01 M HNO_3. The distribution coefficients (Table 10) show that the plutonium adsorption decreases dramatically as the acid concentrations in the feed solvents increase. Results from the desorption tests show that 30, 70, and ~90%, respectively, of the plutonium from the MP-1, MP-50, and A-26 resins were eluted in one equal-volume equilibration with 30% TBP--0.70 M HNO_3--dodecane for 1 hr.

The results from the plutonium retention tests indicated that DBP adsorbed along with plutonium on the MP-1 resin, but not on the MP-50 resin.

Table 10. Effectiveness of macroreticular resins in adsorbing plutonium from simulated Purex solvent[a]

Resin	Type of resin	Resin form	Equilibration time (hr)	H^+ conc. in feed solvent (M)	Plutonium DC[b]
MP-50	Strongly acidic cation	H^+	24	0.03	1.5×10^4
MP-50	Strongly acidic cation	H^+	1	0.03	1.9×10^3
MP-50	Strongly acidic cation	H^+	1	0.17	4.1×10^2
MP-50	Strongly acidic cation	H^+	1	0.36	1.2×10^2
MP-50	Strongly acidic cation	H^+	1	0.57	28
MP-50	Strongly acidic cation	H^+	1	0.69	3
A-15	Cation	H^+	1	0.03	28
MP-1	Strongly basic anion	OH^-	24	0.03	2.5×10^4
MP-1	Strongly basic anion	OH^-	1	0.03	1.7×10^4
MP-1	Strongly basic anion	OH^-	1	0.71	15
MP-1	Strongly basic anion	NO_3^-	1	0.03	9
A-26	Weakly basic anion	OH^-	1	0.03	6.7×10^3
A-26	Weakly basic anion	OH^-	1	0.19	44
A-26	Weakly basic anion	OH^-	1	0.40	28
A-26	Weakly basic anion	OH^-	1	0.73	<1
Sm-2	Inert base resin	-	1	0.03	2.75

[a]10 ml of 30% TBP--0.00011 M DBP--0.0038 M Pu--0.03 to 0.73 M HNO_3 in dodecane equilibrated with 1 g of resin at 25°C.

[b]DC = distribution coefficient.

The effluent from the MP-1 resin had a relatively high plutonium retention power, whereas the effluent from the MP-50 resin had a low plutonium retention power.

The following conclusions have been tentatively drawn from the data in Table 10 and from other information available at this time:

(1) Plutonium can be very effectively adsorbed on macroreticular resins from TBP-DBP-Pu(IV)-HNO_3-dodecane solvent systems. DBP adsorbs on some anion resins but not on the cation resin we tested.

(2) The plutonium adsorption reactions are reversible - at least for the MP-50 and the A-26 resins. The plutonium can be eluted by using eluents with high acid concentrations (0.7 M). More work is needed to positively demonstrate the elution of the MP-1 resin.

(3) Strongly basic anion resins would possibly need to be in the OH^- form before they could be effectively used to adsorb impurities from Purex solvents. A low plutonium distribution coefficient (DC) was obtained using MP-1 resin in the NO_3^- form (Table 10).

(4) The kinetics of plutonium adsorption on MP-1, MP-50, and A-26 resin in the TBP-MBP-dodecane solvent system needs to be investigated. Distribution coefficients at 24 hr were significantly greater than at 1 hr (Table 10).

(5) An effective solvent cleanup method using two or more resin columns in series is indicated--a cation column to remove

plutonium and other metal ions and an anion column and/or an inert base resin column to remove organic impurities.

(6) A much more extensive investigation of the use of solid adsorbents for cleanup of recycle Purex solvent is warranted.

Irradiated solvent tests. Preparations are under way to test various solvent cleanup methods on irradiated Purex solvents. A sample of solvent with a relatively long irradiation time, about 15 min, has been obtained from D. O. Campbell of the Chemical Technology Division. A 50-ml sample of this solvent which had been used to extract irradiated fuel feed samples in the hot cells in Bldg. 2026 has a gamma reading of approximately 1 R/hr at contact. Experimental tests with the solvent will be conducted in an alpha glove box with localized lead shielding in Room 127, Bldg. 4501.

3.1.2 Plutonium valence adjustment

M. R. Bennett (Chemistry Division, ORNL)

Final modifications of the apparatus to be employed in evaluating the effectiveness of nitrogen oxide gases (viz., NO, NO_2) in reducing Pu(VI) to Pu(IV) in HNO_3 solutions are being completed. The calibration by wet-test meter of the flowmeters for nitrogen and nitric oxide gases proceeded smoothly; however, in the case of nitrogen dioxide (NO_2), it was necessary to modify the existing apparatus by substitution of a differential pressure (DP) cell heated to 135°C in place of the flowmeter to shift the equilibrium $2NO_2 \rightleftarrows N_2O_4$ to greater than 99% monomer. We have experienced considerable delays in the modifications due to the shortage of available labor in all of the crafts required for the installation. In addition, it was necessary to disassemble and move all of the apparatus from one laboratory

to another due to the unavailability of 100-psi instrument air pressure. Since these problems have now been resolved, we anticipate no further difficulties in completing the remaining installation and operation procedures.

3.1.3 Ruthenium chemistry

L. Maya (Chemistry Division, ORNL)

A high degree of separation of fission products from uranium and plutonium is required in the processing of irradiated fuels. This is usually achieved, except in the case of a few elements. Ruthenium, for example, is among the elements limiting the decontamination factors (DFs) that can be obtained. This has prompted an extensive amount of work in the past, which has resulted in the characterization of the major ruthenium species involved in the system. These species are complexes that have a tightly bound nitrosyl group and any of a combination of the following ligands: NO_3^-, NO_2^-, OH^-, H_2O, and TBP occupying the remaining five positions in the primary octahedral coordination sphere around the metal. The distribution characteristics, as a function of the different parameters of the system, and the kinetics of ligand exchange reactions for these species are known, thus allowing the prediction and control of the behavior of the ruthenium in the Purex process. However, there is a small fraction (of the order of 1% of the ruthenium) composed of uncharacterized compounds which are responsible for the contamination of the solvent and product streams. These compounds apparently originate from two sources. One is a small fraction of highly extractable species, originally present in the

dissolver solution in the form of binuclear or polymeric compounds, while the other is formed in the solvent by the transformation of ruthenium species by complexation with solvent degradation products.

The requirements for processing highly irradiated fuels during the long-term operation of commercial plants necessitate an improvement in the ruthenium DFs over those which can be achieved with presently available knowledge. A better understanding of the nature of the highly extractable species, as well as the development of effective solvent cleanup procedures, is needed. Future experimental work will be directly along these lines.

Preliminary work has been started with the preparation of the pure compounds $RuNOCl_3$, $RuNO(OH)_3$, and $RuNO(NO_3)_3(H_2O)_2$. The first compound was prepared as an intermediate and was not isolated. Analysis of the other two compounds is under way in the Analytical Chemistry Division. The infrared spectrum of $RuNO(NO_3)_3(H_2O)_2$ has been obtained for future reference. A differential ebullioscopy apparatus is being assembled for the determination of molecular weights, to be used along with other methods of analysis in the characterization of purified compounds that might be isolated in the course of this work.

3.1.4 Chemistry of hydroxylamine and hydrazine in the reductive stripping of plutonium

A. D. Kelmers and D. Y. Valentine (Chemistry Division, ORNL)

Reaction of hydroxylamine with nitric acid. In the Purex processing of LWR fuel, the uranium and plutonium are coextracted into a tributyl phosphate (TBP)-diluent organic phase following HNO_3 dissolution and are then partitioned by reductive stripping. In reductive stripping, the plutonium- and uranium-bearing organic phase is contacted with dilute HNO_3

containing a suitable reductant which causes the plutonium to be reduced from Pu(IV) to Pu(III). Plutonium(III) is not complexed by TBP and thus transfers to the aqueous phase, while the uranium remains in the organic phase. Hydrazine-stabilized hydroxylamine nitrate is a practical reductive stripping reagent pair. The hydroxylamine rapidly reduces Pu(IV), although excess hydroxylamine is required to overcome kinetic problems. The hydrazine destroys any nitrous acid present in the nitric acid and/or the TBP-diluent organic phase and, consequently, prevents the nitrous acid from catalyzing the reoxidation of Pu(III) to Pu(IV).

The aqueous solution from the stripping contactors contains Pu(III) and the unreacted excess hydroxylamine. In some Purex processing flowsheets, these solutions are boiled to concentrate the plutonium and to recycle the nitric acid. The reactions of hydroxylamine in such an acid concentrator are not known. The spontaneous decomposition[7] of hydroxylamine may occur:

$$4NH_2OH \rightarrow N_2O + 2NH_3 + 3H_2O, \qquad (1)$$

which would yield N_2O gas and ammonium nitrate in solution. In heated nitric acid, the oxidation reaction

$$4NH_2OH + 2HNO_3 \rightarrow 3N_2O + 7H_2O \qquad (2)$$

was proposed,[8] based on a single experimental gas analysis.

A research effort has been initiated to define the reactions of hydroxylamine during solution concentration. A glass reaction flash with a reflux condenser and reagent addition funnel attached was set up so that it could be heated and the contents stirred and periodically sampled. A 4 M HNO_3 solution was placed in the flask and a sufficient volume of 1 M hydroxylamine nitrate--2 M HNO_3 solution was added to give final concentra-

tions of 0.5 M hydroxylamine nitrate and 3 M HNO_3 in the resulting solution if no reaction occurred. These approximate the concentrations to be found in a plutonium concentrator in the Purex process. In some experiments, the solution was held at a given temperature and the hydroxylamine nitrate was slowly added over a period of 15 to 30 min. In other experiments, the components were mixed cold (10 to 20°C) and then slowly heated for 1 to 2 hr. The contents were periodically sampled and subsequently analyzed for hydroxylamine and ammonia.

The following results were observed:

(1) At temperatures below 40°C, solutions containing hydroxylamine nitrate and nitric acid were indefinitely stable (sampled for periods up to 2 hr) and no reaction occurred.

(2) Hydroxylamine nitrate--nitric acid solutions that were prepared cold were heated in all-glass apparatus to 90°C and held for 2 hr without any reaction occurring. Again, the solutions appeared to be indefinitely stable.

(3) When the HNO_3 solution in the flask was heated to temperatures between 40 and 103°C (reflux temperature) and the hydroxylamine nitrate solution at room temperature was added dropwise to the flask, an immediate reaction occurred with the evolution of gases and brown fumes. The reaction was always vigorous and prompt. The addition of several strips of type 302 stainless steel and uranyl nitrate at a concentration of 340 g of uranium per liter did not inhibit the reaction.

(4) In one test with the stainless steel strips and uranyl nitrate (170 g of uranium per liter) present, the hydroxylamine nitrate

and nitric acid were mixed cold (10°C) and then slowly heated. At about 50°C a reaction, as evidenced by the evolution of gas bubbles and brown fumes, began on the surface of the stainless steel strips and rapidly accelerated, apparently in an autocatalytic manner.

(5) The chemical analyses of samples taken were of limited use. If no reaction occurred, the concentration of hydroxylamine nitrate was not changed. If a reaction occurred, values of 0.001 to 0.003 M hydroxylamine were obtained, which may be an analytical blank value. No evidence for ammonium ions, other than a small value which apparently comes from ammonia in the hydroxylamine nitrate stock solution, probably via reaction (1) on extended storage, was detected after any of the reactions.

Two attempts were made to determine the composition of the reaction gases. In each case, the vapor space in the reaction flask was swept with helium. The helium stream was scrubbed by caustic (either 1 M NaOH or 1.6 M KOH) to remove NO_2, passed through a Drierite bed to remove moisture, and then sent to a liquid nitrogen trap to freeze out NO and N_2O. After completion of the reaction of hydroxylamine nitrate and nitric acid at 100°C, solids of a brilliant blue color (characteristic of N_2O_3) were found in the liquid nitrogen trap. Apparently the caustic scrubber did not remove all of the NO_2; therefore, it combined with NO by the well-known reaction

$$NO_2(g) + NO(g) \rightleftarrows N_2O_3(s), \qquad (3)$$

where (g) and (s) represent the gaseous and solid phases, respectively.

The solids were allowed to warm and expand into a gas sampling bulb and were subsequently analyzed by mass spectroscopy. Only N_2O was detected; the NO and NO_2 that must have been present from the N_2O_3 could not be detected by this technique.

With regard to Purex processing, the following conclusions can be drawn:

(1) Hydroxylamine can be completely decomposed in hot HNO_3, yielding an undefined nitrogen oxide gas mixture.

(2) The reaction is quite vigorous; thus, large volumes of hydroxylamine nitrate in HNO_3 should not be heated since the reaction appears to be autocatalytic and the rate of gas evolution cannot be controlled. Safe operating procedure would dictate the slow addition of hydroxylamine nitrate solutions to a large volume of hot HNO_3 in an apparatus which is able to handle the volume of gases formed.

(3) Since no ammonium ion was formed, the destruction of hydroxylamine must proceed via an oxidation reaction such as reaction (2). In addition to N_2O, the reaction gases contained some NO and NO_2, either from additional undefined hydroxylamine-HNO_3 reactions or reactions of N_2O with hot HNO_3.

Research efforts are now being directed toward development of a gas-chromatographic method for the quantitative analysis of NO_2, NO, H_2O, and H_2 gas mixtures. This will be of value in a number of areas of Purex process research and development.

Preparation of hydrazoic acid solutions. During the reductive stripping of plutonium in Purex processing, hydrazine is added to the

dilute HNO_3 strip solution as a holding reductant in order to prevent the reoxidation of Pu(III) to Pu(IV). Such reoxidation is deleterious to processing since Pu(IV) will be reextracted into the TBP-organic phase; thus plutonium recycle or third-phase formation can occur in the stripping contactors. Hydrazine is effective as a holding reductant because it rapidly destroys any nitrous acid present, the agent responsible for the reoxidation of plutonium. The reaction of nitrous acid with excess hydrazine, the condition prevailing when hydrazine is used as a holding reductant, leads almost stoichiometrically to the formation of hydrazoic acid:[9]

$$HNO_2 + N_2H_4 \rightarrow HN_3 + 2H_2O. \tag{4}$$

Little information is available concerning the chemistry of hydrazoic acid in Purex processing. Hydrazoic acid is reported[10] to extract into the organic phase more strongly than nitric acid and to strip into the sodium carbonate scrub as sodium azide. Additional research is needed for the following purposes: to define the hydrazoic acid distribution coefficients as a function of temperature and of TBP and nitric acid concentrations; to study the reaction of hydrazoic acid and nitrous acid in the organic phase; to investigate the formation of plutonium azide complexes; and to study methods for the destruction of hydrazoic acid.

Initially, methods for the preparation and handling of standard hydrazoic acid solutions must be developed. While dilute hydrazoic acid solutions are stable, aqueous solutions with a concentration higher than 20% are unstable and may explode unpredictably. Because of the low boiling point (37°C), a portion of the hydrazoic acid distributes to the

vapor phase; however, it should not be allowed to concentrate since gaseous HN_3 is very explosive. Ion exchange techniques have been reported[11] for the safe preparation of hydrazoic acid from sodium azide (NaN_3).

In order to prepare solutions of HN_3, the following test was carried out. A Pyrex column 2 cm in diameter and about 30 cm long was plugged with 5 cm of glass wool and filled with wet IR-120 Amberlite resin that had been previously equilibrated with a 10% H_2SO_4 solution rinsed with distilled H_2O. About 70 ml of NaN_3 was passed through the column over about a 5-min period to form hydrazoic acid by the reaction

$$NaN_3 + RzSO_3H \rightleftarrows RzSO_3Na + HN_3. \tag{5}$$

The column was spent when the reddish-brown color of the Fe(III) complex [Fe(III) ion is a common impurity in NaN_3] was detected on the glass wool plug. The column was repeatedly regenerated with H_2SO_4, and further batches of HN_3 were prepared. The Analytical Chemistry Division is developing an analytical method based on the iron azide colored complex. Analyses of standard solutions will permit an investigation of the stability of hydrazoic acid solutions with regard to oxidation. Once we are able to routinely prepare and analyze stable solution, work on the chemistry of hydrazoic acid in the Purex process can begin.

Reaction of ammonium nitrate and nitric acid. During Purex processing, ammonium nitrate may be formed by the self-oxidation-reduction reaction[9]

$$3N_2H_4 \rightarrow N_2 + 4NH_3, \tag{6}$$

as a by-product in the reaction of hydrazine with nitrous acid:[12]

$$7N_2H_4 + 12HNO_2 + HNO_3 \rightarrow NH_4NO_3 + HN_3 + 5N_2 + 6N_2O + 18H_2O \tag{7}$$

or with nitric acid:[13]

$$17N_2H_4 + 16HNO_3 \rightarrow 4NH_4NO_3 + 4HN_3 + 4N_2O + 11N_2 + 32H_2O. \tag{8}$$

The presence of ammonium ions in reductive stripping solutions containing hydrazine has been reported.[14] If ammonium nitrate is formed, it may be destroyed in nitric acid concentration steps by the reported reaction[15]

$$2NH_4NO_3 + 2NO_2 \rightarrow 3N_2O + 4H_2O + \frac{3}{2} O_2, \qquad (9)$$

where the NO_2 comes from the decomposition of nitric acid.

A series of experiments was carried out to investigate the stability of ammonium nitrate in HNO_3 solutions as a function of temperature and HNO_3 concentration. A glass reaction flask was equipped with a glass condenser and was set up so the contents could be stirred and heated. Strips of 302 stainless steel were included in the flask to simulate process equipment. Solutions of 0.1 M NH_4NO_3 were prepared in 1.0 to 15.5 M HNO_3. The solutions were heated from room temperature to reflux (98 to 103°C) over a 2-hr period and refluxed for 1/2 to 2 hr. Samples were periodically taken and subsequently analyzed for ammonium ion. Contrary to the published[15] reaction (9), no decrease in the ammonium nitrate concentration was observed. It may be that the reagent-grade nitric acid used in these tests was too pure to duplicate the published results.

In the presence of traces of chloride, a fast reaction is reported[15,16] in which nitrosyl chloride acts as a catalytic intermediate. The overall stoichiometry is reported to be:

$$NH_4NO_3 \rightarrow 2H_2O + N_2O.$$

In one test with 0.1 M NH_4NO_3 in 15.5 M HNO_3, 0.05 M HCl was added and the solution was heated to reflux. Again, the ammonium ion concentration did not decrease.

Additional work is needed to explain the apparent stability of ammonium nitrate in HNO_3 solutions containing chloride. Of course, in the Purex process, chloride must be excluded to protect the stainless steel containment. Thus, the present results, if substantiated, suggest that ammonium nitrate may not be destroyed in acid concentration steps.

3.1.5 Plutonium extraction studies

R. H. Rainey, J. H. Paehler, and J. T. Barker (Chemical Technology Division, ORNL)

Six jacketed separatory funnels for studying extraction coefficients have been made and mounted in a rack. The required motors, stirrers, and controlled-temperature water circulator have been purchased and connected. Uranyl nitrate solutions and purified 6% TBP in n-dodecane (NDD) solutions were prepared; uranium extraction coefficients as a function of uranium concentration, HNO_3 concentration, and temperature will be made to check out the equipment and techniques.

Two glove boxes have been cleaned in preparation for solvent extraction work using plutonium.

3.2 Purex Studies with Irradiated Fuels

V. C. A. Vaughen (Chemical Technology Division, ORNL)

Current work with irradiated fuels is described in Sect. 2.2, based on batch extraction work. The solvent extraction system for continuous studies will be installed in TRU. The major accomplishments this quarter have been in the area of establishing the program goals and staffing requirements and in initiating the construction of the Purex Flowsheet Test Facility.

3.2.1 Purex process studies

H. C. Savage (Chemical Technology Division, ORNL)

A preliminary equipment flowsheet for the small-scale, Purex hot-cell solvent extraction system for installation in Cell 5 at TRU is shown in Fig. 8. As seen, the system consists of three banks of ORNL mixer-settlers of the type previously used in the CRF. This first flowsheet utilizes existing equipment (e.g., Zircaloy pit tanks of 25-liter capacity) and may be modified later. The feed solution and product storage tanks shown in Fig. 8 are sized to allow up to 24 hr of continuous operation based on a set of chemical flowsheet parameters determined by the SEPHIS program and listed in Table 11. The maximum operating time shown is 28 hr, which is required to reach 99.9% of steady state in the partitioning column (Table 12). The time required to achieve 99.9% of steady state in the extraction and stripping columns is 5 hr or less. The 24 hr of continuous operation was chosen as a basis for the preliminary flowsheet to provide flexibility of operation and to permit the use of tank sizes that are not excessively large (~5 to ~100 liters).

Purchase orders have been issued for the fabrication and assembly of three additional 16-stage ORNL mixer-settlers (stage volume, ~60 ml) for use in the hot cell and three 16-stage SRL miniature mixer-settlers (stage volume, ~16 ml) for use in the laboratory. Drive motors and speed controllers required for operation of the mixer-settlers have been purchased and received. Both types of mixer-settlers will be evaluated in cold tests. ORNL units will be used in the hot-cell facility because (1) calculations indicate that the operating time required to reach steady state is about one-half that required for the SRL units; (2) all 16 settler

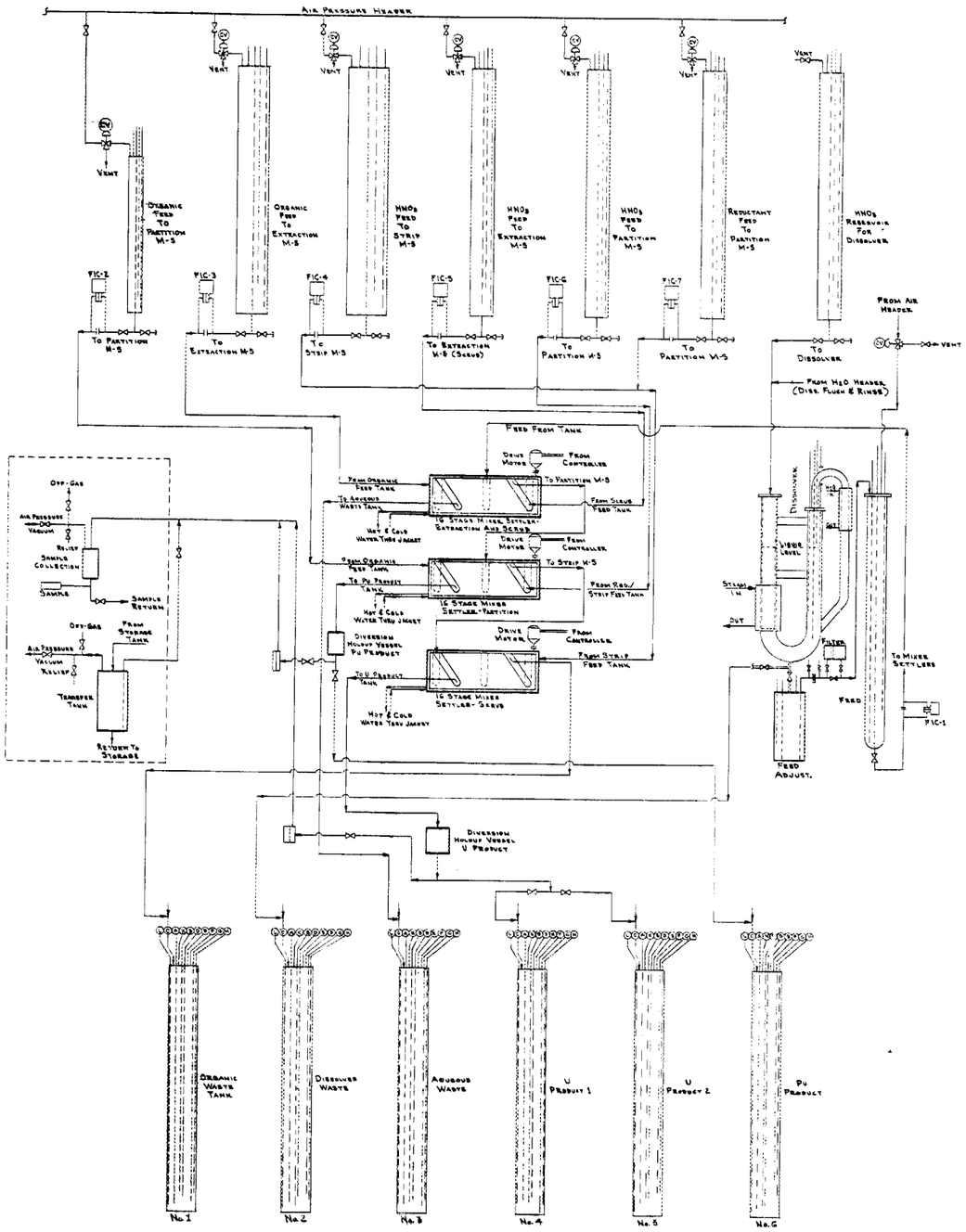

Line Identification (Typ. All Tanks)
A: Off Gas
B: Sample Suction
C: Soln. Add. & Sample Return
D: Air Stage
E: Decontamination Spray
F: Liquid Level & Density
G: Liquid Level & Density
H: Liquid Level & Density
K: Soln. Removal
L: To Waste System

LWR Fuel Reprocessing Flowsheet
Tabulation Of Process Vessels, Flow Rates

Identification	Dissolver	Feed Adjust.	Feed	Aqueous Waste	Pu Product	U Product #1	U Product #2	TBP Feed #1	TBP Feed #2
Location	In-Cell	In-Cell	In-Cell	Pit	Pit	Pit	Pit	Chem. Make-Up	Chem Make-Up
Size	3" Diam.	6" Diam.	4" Diam.	6" Diam.	6" Diam.	6" Diam.	6" Diam.	6" Diam.	3" Diam.
Volume	~8 ℓ	~14 ℓ	~10 ℓ	~25 ℓ			~25 ℓ	~34 ℓ	~4.8 ℓ
Material	304SS	304SS	304SS	Zr			Zr	304SS	304SS

Identification	Strip Feed	Scrub Feed	Partition Feed (HNO3)	Reductant Feed	Dissolver Feed	Org. Waste Diss Waste			
Location	Chem Make-Up	Chem Make-Up	Chem Make-Up	Chem Make-Up	Chem Make-Up	Cell Pit			
Size	8" Diam.	4" Diam.	4" Diam	4" Diam	4" Diam	Existing			
Volume	~50 ℓ	~10 ℓ	~10 ℓ	~10 ℓ	~10 ℓ	~25 ℓ			
Material	304SS	304SS	304SS	304SS	304SS	Zr			

Line No.	Function	Flow Rate ml/min	Solution Composition
24	M-S Strip (1CX)	0-67	Aqueous, 0.3 M HNO3
23	M-S Strip (1Bex)	0-5	Aqueous, 7.8 g/ℓ Pu, 1.5 M H+
20	M-S Scrub (1Bsc)	0-5	Organic, 30% TBP-NDD
19	M-S Scrub (1AS)	0-5	Aqueous, 3.0 M HNO3
15	M-S Feed (1AF)	0-10	Aqueous, 300 g/ℓ U, 3.0 g/ℓ Pu
16	M-S Strip (1AX)	0-30	Organic, 30% TBP-NDD
25	Waste (1CW)	0-30	Organic
23	Dissolver Waste	—	Aqueous
18	Raffinate (1AW)	0-15	Aqueous
26	Uranium Product (1CU)	0-70	Aqueous
21	Pu Product (1BP)	0-5	Aqueous

Fig. 8. Purex process (preliminary hot-cell flowsheet).

Table 11. LWR hot-cell Purex solution flows

Basis: Each mixer-settler stage = 60 ml; maximum throughput = 100 ml/min

Stage	Designation		Phase composition	Temp. (°C)	Flow ratio	Maximum flow rate (ml/min)
			Chemical Flowsheet			
1	1CX	Aqueous:	0.3 N HNO_3	43	6.5	67.0
15	1BSt	Aqueous:	7.55 g Pu/liter, 1.5 M H^+	43	0.4	4.1
28	1BSc	Organic:	30% TBP--NDD	25	0.2	2.1
29	1AS	Aqueous:	3.0 N HNO_3	25	0.2	4.1
36	1AF	Aqueous:	300 g U/liter, 3.0 g Pu/liter	25	1.0	10.3
42	1AX	Organic:	30% TBP--NDD	25	3.0	31.0
			Output Streams			
1	1CW	Organic:	<0.01 g U/liter, <0.01 g Pu/liter, 0.03 N H^+	43	3.2	33.0
14	1CU	Aqueous:	45.4 g U/liter, <0.001 g Pu/liter, 0.32 N H^+	30	6.6	68.0
15	1BU	Organic:	90.5 g U/liter, <0.001 g Pu/liter, 0.1 N H^+	25	3.3	34.0
28	1BP	Aqueous:	<0.01 g U/liter, 7.4 g Pu/liter, 1.9 N H^+	25	0.4	4.2
29	1AP	Organic:	96.5 g U/liter, 0.97 g Pu/liter, 0.15 N H^+	25	3.1	32.0
42	1AW	Aqueous:	<0.01 g U/liter, <0.001 g Pu/liter, 2.49 N H^+	25	1.3	13.3

Table 12. Times required to reach 90 to 99.9% of steady state in mixer-settlers[a]

Contactor	Section	Displacement time[a] (min)	Time (hr) to reach % of steady state				
			90%	95%	99%	99.5%	99.9%
A	Scrub	1.7	1.2	1.2	1.6	2.3	5
	Extraction	1.4	0.9	1.0	1.2	1.8	3.9
B	Scrub	9.5	6.8	7.0	9.2	13.1	28.5
	Partition	1.6	0.9	1.2	1.5	2.2	4.8
C	Strip	0.6	0.4	0.4	0.6	0.8	1.8

[a]Based on 60-ml stage volumes and a maximum total flow of 100 ml/min (see flow rates in Table 11).

stages are located on the front side of the mixer-settler, providing direct visual observation of all settlers and easier access for sampling; and (3) these units have been proven in extensive hot-cell operations at ORNL.

3.2.2 Solvent extraction flowsheet development

R. H. Rainey (Chemical Technology Division, ORNL)

A new flowsheet based on SEPHIS calculations was developed for use in cold studies. The flow ratios and concentrations calculated by SEPHIS are shown in Table 13. Coextraction and costripping satisfy the needs of the two mixer-settler banks since no plutonium is presently being used. The main purpose of the current series of test runs is to determine the operating characteristics of the mixer-settler units under various conditions of flow rates, flow ratios, and impeller speeds. The run conditions and results obtained thus far are detailed in Sect. 3.3. An interesting facet of this work is that when 0.3 M HNO_3 was used as the strip solution (to prevent plutonium polymerization in an actual hot run) the flow ratio of strip to organic (over the ratio for a flowsheet using 0.1 M HNO_3 as strip) had to be increased by nearly a factor of 2 in order to attain calculated losses less than 0.01%.

Table 13. Flow ratios and concentrations calculated by SEPHIS

Stream	Code	Flow ratio	Calculated concentration	
			U (g/liter)	HNO_3 (M)
Pregnant organic	1AP	3.64	82.5	0.24
Strip	1CX	8.00	0	0.30
Used solvent	1CW	3.50	<0.01	0.03
Uranium product	1CP	8.11	36.9	0.39

In other work, comparisons between the experimental and calculated concentrations of uranium and acid in countercurrent batch extraction experiments (see Sect. 3.3) were made to determine where there were probable analytical errors. These are being rechecked. One may use the calculations to estimate the extent of steady state attained in the batch experiments.

3.3 Cold Studies

W. D. Bond, F. A. Kappelmann, and F. M. Scheitlin
(Chemical Technology Division, ORNL)

Work performed this quarter consisted of mixer-settler extraction studies and measurements of the equilibrium distribution of uranium, HNO_3, and key fission products.

3.3.1 Mixer-settler extraction studies

A 12-hr run with a feed solution 2.5 M in HNO_3 and containing 306 g of uranyl nitrate was made using two 16-stage mixer-settler banks. The purpose of the run was to evaluate the effectiveness of the mixer-settler units in extracting and stripping the uranium. A temperature of 42 to 43°C was used in both the extraction and stripping banks. The flowsheet employed was based on SEPHIS calculations and was provided by R. H. Rainey. Flowsheet conditions were as follows:

Extraction Bank - Feed: 306 g of uranium per liter in 2.5 M HNO_3 at 0.5 liter/hr.

Solvent: 30% TBP--dodecane at 1.75 liters/hr.

Scrub (8 stages): 3 M HNO_3 at 0.2 liter/hr.

The organic phase from the extraction bank was stripped with 0.3 M HNO_3 flowing at 4.0 liters/hr.

To avoid phase disengagement difficulties with the stripping bank, it was necessary to use a split flow of the stripping solution. The stripping solution was metered to stage 1 at 0.5 liter/hr and to stage 5 at 3.5 liters/hr. The uranium-laden solvent from the extraction bank entered stage 16 of the stripping bank.

Operations with both mixer-settler banks were generally satisfactory. Samples of the aqueous and organic streams exiting the extraction and stripping banks were taken for uranium and HNO_3 analyses at 1-hr intervals during the run. Aqueous and organic samples were taken from each stage on completion of the run. Equilibration shakeout tests were also performed for each stage at the end of the run. Recovery data based on the stripped product solution were as follows:

Extraction raffinate: 0.00035 g U/liter x 10.8 liters = 0.0038 g of uranium

Stripped organic: 0.0055 g U/liter x 21.5 liters = 0.118 g of uranium

Aqueous product: 37.5 g U/liter x 50.8 liters = 1905 g of uranium

Percent loss: 0.0066

Percent recovery: 99.993

Analyses pertaining to approach of the banks to steady-state conditions and to the stage efficiency of the banks are incomplete at this time.

3.3.2 Batch countercurrent extraction studies

Extraction experiments are being carried out to generate equilibrium distribution coefficient data for the extraction of uranium, plutonium, and key fission products into TBP. These data will increase our confidence in calculations made using the SEPHIS code. Work to date has consisted of experimental studies on the extraction of uranium, zirconium, ruthenium,

and molybdenum from both HNO_3 and simulated LWR dissolver solutions. Installation of equipment in a glove box for plutonium extraction studies is nearly complete.

Four extraction stages and three scrubbing stages were employed in countercurrent extraction experiments; seven stripping stages were used in stripping experiments. Five extraction experiments and two stripping experiments have been carried out to determine the distribution of uranium and HNO_3 between the aqueous and organic phases. The experimental results obtained do not agree with SEPHIS calculations, and the discrepancy has been traced to faulty analysis of HNO_3. The experimental results shown for one of the stripping experiments (Table 14) are typical of those obtained thus far. Work on obtaining reliable analyses of HNO_3 is currently in progress.

Several experiments have been conducted to determine the distribution of zirconium, ruthenium, and molybdenum in the extraction and scrubbing stages. In the early runs we used the SSMS method to detect the elemental distribution. However, this approach was unsuccessful because of the low elemental concentration in the organic phase, particularly in the scrubbing stages.

Radioactive tracers are currently being used to determine the distribution of the fission products. Two zirconium extraction runs have been made in which fission products were present in concentrations expected in the high-activity solvent extraction feed. Results are shown in Table 15. The extraction behavior generally agreed with that expected from literature data.[17]

Table 14. Comparison of experimental distribution of uranium and HNO_3 with values calculated by the SEPHIS Code

Aqueous strip: 0.126 M HNO_3; volume entering stage 7 = 33 ml
Organic feed: 28.8% TBP, 87.8 g U/liter--0.066 M HNO_3; volume entering stage 1 = 30 ml

Stage number	Organic phase				Aqueous phase			
	HNO_3 (M)		Uranium (g/liter)		HNO_3 (M)		Uranium (g/liter)	
	Exptl.	SEPHIS	Exptl.	SEPHIS	Exptl.	SEPHIS	Exptl.	SEPHIS
1	0.14	0.001	74.8	72.8	0.40	0.127	66.9	72.4
2	0.16	0.009	67.0	60.8	0.50	0.126	58.4	58.7
3	0.17	0.01	59.5	50.7	0.32	0.126	49.2	48.0
4	0.19	0.01	49.8	40.9	0.26	0.125	39.8	39.0
5	0.21	0.016	38.3	30.5	0.24	0.124	31.6	30.4
6	0.14	0.016	28.3	18.6	0.22	0.126	23.4	21.1
7	0.02	0.009	13.8	6.6	0.19	0.174	13.5	10.5

Table 15. Countercurrent extraction of zirconium from simulated fission products

Aqueous feed: Simulated fission products in 2 M HNO_3; volume entering stage 4 = 15 ml
Organic: 30% TBP; volume entering stage 1 = 30 ml
Scrub: 2 M HNO_3; volume entering stage 7 = 15 ml

Stage number	Distribution coefficient	
	2-min contact	10-min contact
1	0.030	0.039
2	0.040	0.046
3	0.040	0.045
4	0.035	0.034
5	0.083	0.076
6	0.073	0.054
7	0.14	0.093

4. OFF-GASES - FLUOROCARBON ABSORPTION STUDIES*

W. S. Groenier
(Chemical Technology Division, ORNL)

This program is concerned with the development of the Krypton Absorption process on an accelerated basis. Funding is provided for expansion of the pilot-plant development, initiation of plant engineering design criteria, performance of a proposed system reliability analysis, and a study of the chemical effects of impurities in the fluorocarbon solvent on the process and equipment.

4.1 Fluorocarbon Absorption Process Development

M. J. Stephenson (ORGDP)

4.1.1 Pilot-plant operation

M. J. Stephenson, R. S. Eby, V. C. Huffstetler, and B. E. Kanak (ORGDP)

The remaining pilot-plant tests scheduled under campaign 3 have been completed. This work was directed toward further defining the general process disposition of the various feed gas components, including carbon dioxide, nitrogen dioxide, iodine, methyl iodide, water, and xenon, and the effects of these components on the operability and overall performance of the process. Test results with nitrogen dioxide, iodine, and methyl iodide were reported previously.[6] Work with carbon dioxide and xenon is reported here. Pilot-plant tests with water have been rescheduled for the next experimental campaign because the necessary analytical equipment was not available during this operating period.

---

*Jointly funded by LWR Recycle and LMFBR Reprocessing programs.

The results of the carbon dioxide and xenon removal tests are summarized in Fig. 9; krypton data are included for comparison. The absorption step was conducted at a pressure of 300 psig and a temperature between -25 and 0°F in these runs. An infrared gas analyzer was used to establish carbon dioxide removals while gamma scintillation equipment gave the corresponding xenon concentrations. Only tracer levels of activity (e.g., 1 to 3 Ci of ^{133}Xe) were used during the xenon tests. Xenon and carbon dioxide absorber removals in excess of 99.99% were measured in pilot-plant tests that were conducted at the same absorber conditions of pressure, L/G ratio, and temperature that yielded about 99% krypton removal. Carbon dioxide removals were slightly higher than those measured for xenon, consistent with the component solubilities. Based on pilot-plant data, H_{OG} values for Xe and CO_2 were 6 to 10 in. The final stripper column was operated at 15 psig with varying L/G ratios. Measurable amounts of carbon dioxide and xenon were found in the recycle solvent for those tests in which stripper L/G ratios were greater than 2.0; however, the absorber performance was only slightly affected by this recycle in those cases where the process removals exceeded 99.99%. At lower stripper boilup rates (e.g., even when the resulting L/G ratio was as high as 3.0), krypton was not detected in the recycle solvent. This observation is also consistent with component solubilities.

Based on the results of the third pilot-plant operating campaign and other considerations, several pilot-plant modifications were identified as being desirable to improve the efficiency and effectiveness of the process. Most of the flowsheet changes were made this quarter. Specifically, the packed height of the absorber column was increased from 9 ft to 15 ft, an

G-76-1071

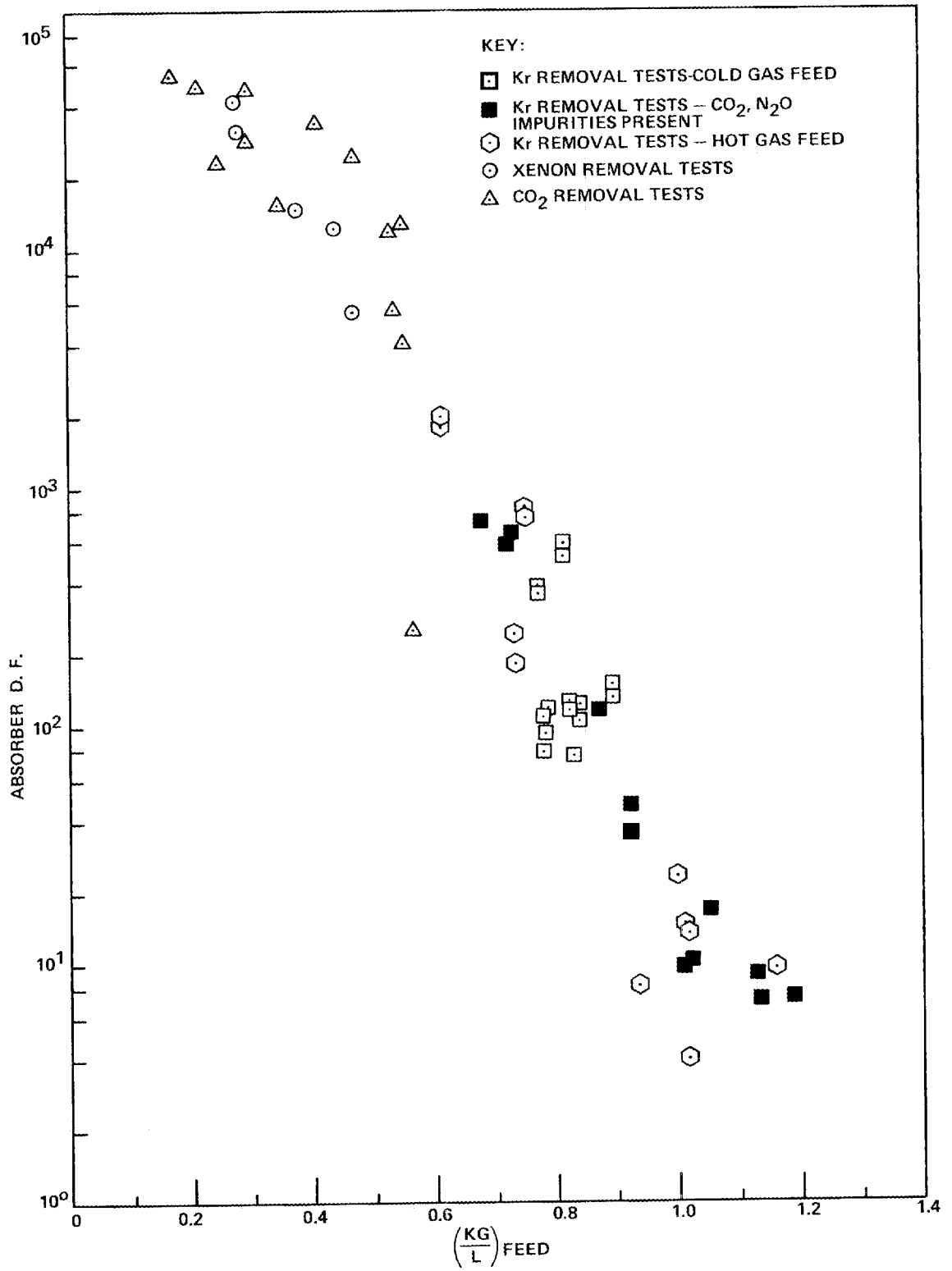

Fig. 9. Summary of recent pilot-plant tests with krypton, xenon, and carbon dioxide (9.0-foot absorber column, 300 psig, and 0°F).

absorber feed gas cooler/desublimer was built and installed in the absorber feed gas line, and solid-state reboiler heater controllers were installed on the fractionator, stripper, and solvent still reboilers. More contacting stages in the absorber will allow the use of lower solvent-to-gas flow ratios, which will improve the overall efficiency of the process. The feed gas cooler/desublimer will permit evaluation of the effectiveness of cold trapping feed gas components such as nitrogen dioxide, water, and iodine. The heat exchanger is fitted with an external gamma scanner for determining iodine loading profiles and has provisions for washout and regeneration. The solid-stage reboiler controllers give automatic heater control capability; manual controls were previously used. The boilup rate of the fractionator is controlled by a selected temperature point on the packed column, the stripper by the column ΔP, and the solvent still by the reboiler liquid level. The automatic heater controls will allow for better compensation of process transients. Digital output wattmeters capable of $\pm$ 1/4% power measurements have been installed on all three reboilers to give a better account of system energy requirements. Repiping of the solvent still to permit better reflux control is the only pilot-plant modification identified through the experimental program that remains to be accomplished. This work is in progress.

4.1.2 Process application

Process modeling studies are continuing. At present, individual process components are being examined in the light of present theory and available data. Heat exchanger calculations, summarized in Fig. 10, show that the feed gas cooler/desublimer will remove high concentrations of water and

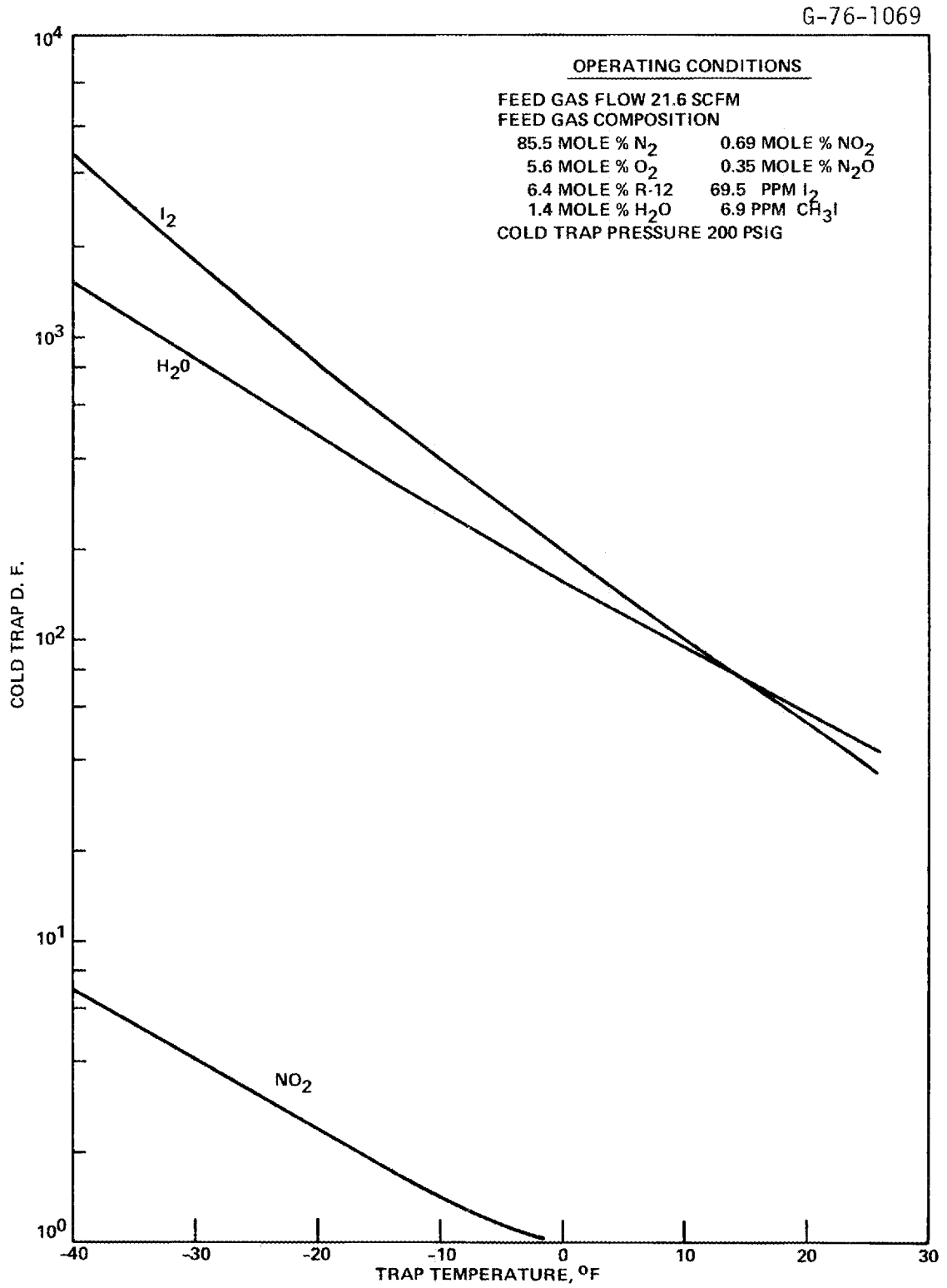

Fig. 10. Calculated cold trap removals of various feed gas components as a function of trap temperature.

iodine. In this case, the cold trap pressure was taken as 200 psig and the effect of various operating temperatures investigated. At the nominal operating temperature of the absorber (i.e., -25 to 0°F), water and iodine removals are predicted to be between 99 and 99.9%. The inlet water and iodine concentrations were assumed to be 1.4 mole % and 69 ppm respectively. With a nitrogen dioxide inlet concentration of 0.69 mole %, only a small quantity of this component would be condensed. Higher operating pressures will decrease the equilibrium partial pressures of the individual feed gas components and hence increase their removal.

In view of the relatively low water solubility limit of the solvent at the temperature of the process and the possible corrosion problems that could develop if large amounts of free water are present,[6] the function of the feed gas cooler/desublimer might prove necessary to ensure the overall plant operation and integrity by greatly reducing the amount of water that might otherwise contact the solvent. Also, the bulk amount of the iodine fed to the process would end up in the heat exchanger and thereby minimize the amount of iodine in the liquid circuit.

In moving toward the objectives of identifying preferred process equipment for the demonstration plant, available gear- and turbine-type solvent pumps are being reviewed. Use of this type of pump would eliminate inherent hydraulic problems associated with the popular liquid-end diaphragm metering chemical pump now used in the pilot plant and significantly reduce process maintenance requirements. Because of head limitations, two or more of the gear or turbine pumps will be needed in series to achieve the absorption pressures required by the process. After the alternate pump has been selected, it will be installed in the pilot plant for evaluation. Also,

since this type of pump has no built-in metering capability similar to that of the diaphragm unit, development of a suitable means of flow control will be required.

4.2 Chemical Studies of Contaminants in LWR Off-Gas Processing

L. M. Toth, D. W. Fuller, and J. T. Bell (Chemistry Division, ORNL)

The chemical research on LWR off-gas components in R-12 refrigerant has been concerned with two major topics during this quarter: (1) the corrosion of the 304 stainless steel vessel by R-12 solutions containing iodine and water, and (2) the general physical and chemical behavior of methyl iodide in the R-12 system.

The corrosion experiments were initiated during the last reporting period. A first-order rate of I_2 loss at 0°C was observed when 50 to 100 ppm of water was added to the R-12 solution, and the rate expression[6]

$$\frac{d(I_2)}{dt} = - k't \qquad (1)$$

was proposed because of the limited solubility of water in R-12. At that time, we suggested that it might therefore be possible to obtain useful fundamental data on 304 stainless steel corrosion in the small-scale spectrophotometric system. We attempted to demonstrate that the rate of I_2 loss was independent of the amount of added water as long as the R-12 solution remained saturated with water, but found that inadequate mixing in our system produced a reaction mechanism which was apparently diffusion controlled. The work was temporarily postponed until a more sophisticated mechanism was constructed. This system has recently been completed, and corrosion measurements will be resumed during the forthcoming months.

Attention was directed at the general physical and chemical behavior of CH_3I in R-12. Methyl iodide was found to be miscible in R-12 up to a concentration of 2.3 moles/liter. It forms stable solutions in R-12 and does not attack the 304 stainless steel container. By monitoring the electronic absorption band of CH_3I at 256 nm and 257 nm (molar extinction coefficient = 230 ± 50 liter $mole^{-1}$ cm^{-1}) in the liquid and vapor phases, respectively, a mole fraction distribution coefficient, $D = x_\ell/x_v$, for the -40 to +300°C range was measured and was fit by least squares to the expression

$$\log_{10}(D) = -1.1 + 476/T, \qquad (2)$$

where T is temperature in K. These data are preliminary and are thus subject to revision after our final measurements are complete. Because CH_3I shows no solubility limits, no saturation data (as was given for I_2) are available.

Design and construction have begun on a simple exhaust system which will satisfy safety requirements for handling nitrogen dioxide in our spectrophotometric system. Experiments incorporating nitrogen dioxide in the R-12 system are expected to begin during the fall quarter upon completion of the installation of safety equipment.

4.3 Reliability Studies

W. E. Unger (Chemical Technology Division, ORNL) and
D. E. Wood* (Kaman Sciences Corporation)

Kaman Sciences Corporation has completed the subcontract (P.O. ORNL 11 X 81721, Reg. UCN-1127) with the issuance of their final report,

---

*Senior Research Scientist, Nuclear Services Program, Kaman Sciences Corp.

"Availability Analysis of the Selective Absorption Pilot Plant," KSC-6212-1.

A summary of this report is provided below.

"Retention of krypton from nuclear fuel reprocessing plants is expected to be required by the early 1980's. A pilot plant, based on absorption in a fluorocarbon, has been constructed at Oak Ridge to develop and test methods for separation of krypton from the off-gas of fuel reprocessing plants. The current study is an analysis of the reliability of the pilot plant, including modifications proposed for use in a future demonstration plant.

Availability was chosen as the measure of success, since the plant can remove most of the krypton even with occasional outages, as long as the outage time is short. This led to the extensive use of standby equipment and bypasses instead of full on-line redundancy.

The GO methodology, developed at Kaman Sciences Corporation, was used for modelling and analysis. In this technique the system diagram is converted to a GO chart by representing each component by an equivalent GO symbol. Connections are represented by logic event numbers and the probabilities are computed from the probabilities of previous events. The computation starts with gas at the input and proceeds through the system to compute success probabilities of intermediate and final events. Sensitivities and system impacts are computed for component kinds to provide a ranking of important components, which might need more accurate data, better components, or redesign with redundancy or bypass. Operator effects can be included.

The calculations were made for six variations of the system model with increasing levels of redundancy and bypass. The total system unavailability, expressed as expected average outage time per year, was reduced from 139 hours in the initial model to 15 hours in the final model.

The bypass model included the effect of an operator performing the bypass and starting the standby unit. The bypass has the effect of reducing the repair time of the system to the relatively short time required to bypass a component or startup a standby unit.

Several conclusions can be drawn from the overall results.

1. The expected outage time of 15 hours will exceed the krypton removal requirement (90%) by a large

enough factor so that more accurate failure data and/or additional redundancy should not be necessary.

2. Occasional failures can be tolerated since short repair time is just as important as low failure rate in minimizing total outage time. Thus standby redundancy (with a short outage for standby startup) is adequate instead of on-line redundancy or automatic switching to eliminate the system failure.
3. Availability of standby units nearby for quick replacement or in-place (ready to start) is important to reduce outage time.
4. Standby units need not be as reliable as the primary unit since the reliability of the standby system depends on correct operator action.
5. The availability of a component and its bypass will be one or two orders or magnitude better than the component alone for the normal range of operator reliability of 0.9 to 0.99. Higher availability could be achieved with automatic switching or on-line redundancy, but this was not necessary in the current study.
6. Long outages, even though rare, should be avoided since the krypton retention limit could be exceeded during the particular year when the outage occurs. Thus complex equipment like the columns should have enough parts available for fabrication and installation in a few days, although a complete spare would not be necessary.
7. Access for repair is important to minimize outage time.
8. Items beyond the still output may need provision for purging and recycling the gas, isolation of sections to reduce the amount to be recycled, and access for contact maintenance, if possible.
9. Product storage should be in units small enough so that a failure would release substantially less than 10% of the year's production."

4.4 Engineering Design Criteria Studies

(No report this quarter.)

5. FINISHING PROCESSES - MOX FUEL FABRICATION

R. B. Fitts, A. R. Olsen, and J. D. Sease
(Metals and Ceramics Division, ORNL)

The objective of this program is to provide technical assistance to SRL in the development of an overall plan in support of LWR-MOX fuel fabrication processes and facilities.

During the quarter, two review meetings were held at ORNL for SRL management. On July 28, R. T. Huntoon and J. T. Buckner, Jr., reviewed the current status of the program and suggested modifications to the program. On September 17, the status of the modified program was reviewed with R. T. Huntoon.

At the request of the Rocky Flats Plant, we provided preliminary review of a draft of their proposed program on conversion processes. While endorsing the method proposed for process evaluation and comparison, we did offer some suggestions on certain features.

5.1 MOX Fabrication Processes

A. R. Olsen (Metals and Ceramics Division, ORNL)

A draft copy of a report surveying the present status of MOX fabrication processes and identifying areas in which research and engineering development efforts are needed was transmitted informally to SRL. At their request, no additional effort will be expended on this general survey at this time.

5.2 MOX Fabrication Facilities

5.2.1 Effects of plutonium radiation characteristics on containment criteria

K. A. Williamson and J. E. Rushton (Metals and Ceramics Division, ORNL)

An essential feature of the design criteria for the MOX Commercial Demonstration Fabrication Facility (CDFF) is establishing the requirements for protecting operational personnel from penetrating radiation. A draft of a preliminary assessment indicating that significant shielding would be required for all fabrication processes involving plutonium with isotopic distributions typical of high-burnup LWR fuels was given to the SRL representatives. A more comprehensive literature search for operating experience is in progress. An annotated bibliography is in preparation and a preliminary report will be published next quarter.

5.2.2 Remote manipulator and viewing development

W. R. Hamel and R. C. Muller (Metals and Ceramics Division, ORNL)

Although a detailed study of the MOX-CDFF requirements for remote manipulation and viewing cannot be undertaken until process and equipment flowsheets are defined, there will be a need to develop improved general manipulation for some process functions and for maintenance activities. Toward this end, design has been started on instrumentation required to provide position control to replace the existing rate control on a commercial electromechanical manipulator. This design will be tested on an available manipulator located in the existing Thorium Uranium Recycle Facility hot cells.

5.2.3 Development of the powder conveying system

J. E. Mack (Metals and Ceramics Division, ORNL)

Both the quantity and nature of the oxide powders involved in commercial reprocessing and refabrication of LWR recycle fuels require establishment of an efficient and reliable method of handling. At the suggestion of the SRL reviewers, a draft of a program proposal to develop such a powder handling process was prepared. This development will take advantage of the experience accumulated and equipment developed in the HTGR Recycle Program (which has been under way for several years), and will include all adjunct features of the conveying system. Pending approval, the detailed experimental program will be defined next quarter.

6. URANIUM HEXAFLUORIDE CONVERSION

J. H. Pashley (ORGDP)

The collection of information relating the various conversion processes was continued throughout the quarter.

7. ECONOMIC STUDIES

7.1 LWR Recycle Data

E. H. Gift (ORGDP)

Calculations have been made to provide mass balance data for a four-region BWR through successive recycle of self-generated plutonium. The BWR model selected was based on the General Electric-designed Brown's Ferry Plant. Calculations were made using the LEOPARD code,[18] a spectrum-dependent, nonspatial depletion code.

Four refueling regions were assumed to be all initially loaded at 2.19 wt % ^{235}U and were estimated to yield respective burnups of 13,520, 17,570, 21,830, and 27,040 MWd/metric ton. All successive reloads were required to match the 27,040-MWd/MT burnup and were loaded to 2.6 wt % ^{235}U. Plutonium from each of the four initial regions was then assumed to be recycled through four refueling cycles. At the end of each cycle, plutonium from the mixed oxide portion of the reload batch was recovered and mixed with the plutonium from the 2.6 wt % slightly enriched ^{235}U portion of the reload batch. This plutonium (after losses in reprocessing and refabrication and decay of ^{241}Pu) was then mixed with natural uranium to provide the mixed oxide fuel for the succeeding reload batch. The results of these calculations for the initial loading and the first and fourth recycle of plutonium are shown in Tables 16-19 for each of the four reload regions. The required fissile enrichment (^{235}U + ^{239}Pu + ^{241}Pu) of the mixed oxide increased from 2.6 wt % for the first recycle of plutonium to about 2.75 wt % for the fourth recycle. This increase is primarily a

Table 16. BWR fuel needs for self-generated plutonium recycle of a reload region initially discharged at 13,519 MWd/MT

[kg/1000 kg (U + Pu) charged]

			1st Recycle of Plutonium				
			Charged		Discharged		
	Initial Loading 1st Cycle						
Isotope	Charge	Discharge	Mixed Oxide	2.6 wt % Slightly Enriched	Mixed Oxide	2.6 wt % Slightly Enriched	Total
U-235	21.90	10.1939	1.4411	20.59924	0.59816	4.91902	5.51718
U-236	0	1.9709	0	0	0.15064	2.55327	2.70991
U-238	978.10	968.2694	201.2403	771.67906	197.58238	756.24511	953.82750
Pu-239	0	3.5880	3.5521	0	1.56702	3.33731	4.90433
Pu-240	0	1.0010	0.9910	0	0.95378	1.38863	2.34241
Pu-241	0	0.4522	0.4076	0	0.66888	0.78531	1.45419
Pu-242	0	0.09052	0.0896	0	0.38976	0.33933	0.729096
Burnup, MWd/MT	0	13,519	0	0	27,037	27,037	27,037
Total Uranium	1000	980.4342	202.6814	792.2783	198.33118	763.71740	962.05459
U-235, Wt. Frac.	0.0219	0.010397	0.00711	0.026	0.0030160	0.0064409	0.005735
Total Plutonium	0	5.1317	5.0403	0	3.57944	5.85058	9.43002
Frac. Fiss. Pu	0	0.787302	0.785608	0	0.62465	0.70465	0.674284
Fraction Fissile	0.0219	0.014443	0.026000	0.026	0.014036	0.011749	0.0122243
U-236, Wt. Frac.	0	0.0201023	0	0	0.00075954	0.0033432	0.0028168

Table 16 (continued)

	4th Recycle of Plutonium				
	Charged		Discharged		
Isotope	Mixed Oxide	2.6 wt % Slightly Enriched	Mixed Oxide	2.6 wt % Slightly Enriched	Total
U-235	2.50305	16.51831	1.15958	3.94451	5.10409
U-236	0	0	0.25839	2.04744	2.30583
U-238	349.54325	618.80112	343.35959	606.42504	949.78463
Pu-239	5.48413	0	3.01179	2.67616	5.68795
Pu-240	3.03194	0	2.05031	1.11352	3.16383
Pu-241	1.92758	0	1.62894	0.62973	2.25867
Pu-242	2.19062	0	2.55499	0.27211	2.82710
Burnup, MWd/MT	0	0	27,037	27,037	27,037
Total Uranium	352.04630	635.31943	344.77756	612.41699	957.19455
U-235, Wt. Frac.	0.00711	0.026	0.0033633	0.0064409	0.0053323
Total Plutonium	12.63427	0	9.24603	4.69152	13.93755
Frac. Fiss. Pu	0.586635	0	0.50192	0.70465	0.570159
Fraction Fissile	0.0271875	0.026	0.016384	0.011749	0.0134387
U-236, Wt. Frac.	0	0	0.00074944	0.0033432	0.0024089

Table 17. BWR fuel needs for self-generated plutonium recycle of a reload region initially discharged at 17,574 MWd/MT.

[kg/1000 kg (U + Pu) charged]

Isotope	Initial Loading 1st Cycle		1st Recycle of Plutonium				
			Charged		Discharged		
	Charge	Discharge	Mixed Oxide	2.6 wt % Slightly Enriched	Mixed Oxide	2.6 wt % Slightly Enriched	Total
U-235	21.90	7.9297	1.6017	19.98957	0.66859	4.77343	5.44202
U-236	0	2.3169	0	0	0.17370	2.47771	2.65141
U-238	978.10	965.1224	223.6771	748.83993	219.61749	733.86306	953.48055
Pu-239	0	3.8560	3.8174	0	1.73553	3.23854	4.97407
Pu-240	0	1.3136	1.3005	0	1.19817	1.34753	2.54671
Pu-241	0	0.6559	0.5913	0	0.76329	0.76206	1.52535
Pu-242	0	0.1843	0.1825	0	0.51911	0.32929	0.84840
Burnup, MWd/MT	0	17,574	0	0	27,037	27,037	27,037
Total Uranium	1000	975.3690	225.2788	768.8295	221.45978	741.11420	961.57398
U-235, Wt. Frac.	0.0219	0.0081299	0.00711	0.026	0.0030327	0.0064409	0.0056595
Total Plutonium	0	6.0098	5.89170	0	4.21610	5.67742	9.89453
Frac. Fiss. Pu	0	0.750757	0.748290	0	0.59269	0.70465	0.65687
Fraction Fissile	0.0219	0.0126777	0.026000	0.026	0.014098	0.011749	0.012292
U-236, Wt. Frac.	0	0.0023754	0	0	0.00078792	0.0033432	0.0027574

Table 17 (continued)

	4th Recycle of Plutonium				
	Charged		Discharged		
Isotope	Mixed Oxide	2.6 wt % Slightly Enriched	Mixed Oxide	2.6 wt % Slightly Enriched	Total
U-235	2.49966	16.52639	1.15935	3.94644	5.10579
U-236	0	0	0.25803	2.04845	2.30648
U-238	349.07004	619.10414	342.88484	606.72199	949.60683
Pu-239	5.50115	0	3.02098	2.67747	5.69845
Pu-240	3.03306	0	2.00099	1.11407	3.11506
Pu-241	1.94545	0	1.63462	0.63004	2.26466
Pu-242	2.32011	0	2.66456	0.27224	2.93680
Burnup, MWd/MT	0	0	27,037	27,037	27,037
Total Uranium	351.56970	635.63053	344.30222	612.71680	957.01910
U-235, Wt. Frac.	0.00711	0.026	0.0033672	0.0064409	0.0053351
Total Plutonium	12.79977	0	9.32115	4.69382	14.01497
Frac. Fiss. Pu	0.581776	0	0.49947	0.70465	0.568186
Fraction Fissile	0.02729696	0.026	0.0164439	0.011749	0.0134587
U-236, Wt. Frac.	0	0	0.00074943	0.0033432	0.00241007

Table 18. BWR fuel needs for self-generated plutonium recycle of a reload region initially discharged at 21,832 MWd/MT

[kg/1000 kg (U + Pu) charged]

Isotope	Initial Loading 1st Cycle		1st Recycle of Plutonium				
			Charged		Discharged		
	Charge	Discharge	Mixed Oxide	2.6 wt % Slightly Enriched	Mixed Oxide	2.6 wt % Slightly Enriched	Total
U-235	21.90	5.9901	1.7082	19.58180	0.73203	4.67617	5.40820
U-236	0	2.5911	0	0	0.18327	2.42722	2.61050
U-238	978.10	961.5779	238.5448	733.56440	232.22718	718.91022	951.1374
Pu-239	0	3.9902	3.9503	0	1.90194	3.17255	5.07449
Pu-240	0	1.5912	1.5753	0	1.22912	1.32007	2.54919
Pu-241	0	0.8427	0.7597	0	0.90156	0.74654	1.64811
Pu-242	0	0.3187	0.3155	0	0.68801	0.32258	1.01059
Burnup, MWd/MT	0	21,832	0	0	27,037	27,037	27,037
Total Uranium	1000	970.15910	240.2530	753.1462	233.87451	726.01361	959.15610
U-235, Wt. Frac.	0.0219	0.0061743	0.00711	0.026	0.00313001	0.0064408	0.0056386
Total Plutonium	0	6.7428	6.60080	0	4.72063	5.56174	10.28224
Frac. Fiss. Pu	0	0.71675	0.71355	0	0.59388	0.70465	0.653807
Fraction Fissile	0.0219	0.0110789	0.026	0.026	0.014818	0.011749	0.012513
U-236, Wt. Frac.	0	0.00267080	0	0	0.00078363	0.0033432	0.0027217

Table 18 (continued)

Isotope	4th Recycle of Plutonium				
	Charged		Discharged		
	Mixed Oxide	2.6 wt % Slightly Enriched	Mixed Oxide	2.6 wt % Slightly Enriched	Total
U-235	2.50235	16.51480	1.15929	3.94367	5.1096
U-236	0	0	0.25841	2.04701	2.30542
U-238	349.44599	618.66996	343.25414	606.29650	949.55064
Pu-239	5.50216	0	3.01986	2.67559	5.69545
Pu-240	2.98326	0	2.03776	1.11329	3.15105
Pu-241	1.94151	0	1.62326	0.62959	2.25286
Pu-242	2.41996	0	2.74366	0.27205	3.01571
Burnup, MWd/MT	0	0	27,037	27,037	27,037
Total Uranium	351.94834	635.18477	344.67184	612.28718	956.95902
U-235, Wt. Frac.	0.00711	0.026	0.0033635	0.0064408	0.00533247
Total Plutonium	12.86689	0	9.42454	4.69052	14.11507
Frac. Fiss. Pu	0.5800679	0	0.49266	0.70465	0.5631081
Fraction Fissile	0.02731761	0.026	0.016387	0.011749	0.01344004
U-236, Wt. Frac.	0	0	0.000749728	0.0033432	0.00240911

Table 19. BWR fuel needs for self-generated plutonium recycle of a reload region initially discharged at 27,037 MWd/MT

[kg/1000 kg (U + Pu) charged]

Isotope	Initial Loading 1st Cycle		1st Recycle of Plutonium				
			Charged		Discharged		
	Charge	Discharge	Mixed Oxide	2.6 wt % Slightly Enriched	Mixed Oxide	2.6 wt % Slightly Enriched	Total
U-235	26.00	6.2087	1.8352	19.10106	0.76752	4.60610	5.37362
U-236	0	3.2227	0	0	0.19124	2.39085	2.58209
U-238	974.00	954.5199	256.2857	715.55514	244.79897	708.13836	952.93733
Pu-239	0	4.2123	4.1702	0	1.98543	3.12502	5.11045
Pu-240	0	1.7527	1.7352	0	1.29005	1.30029	2.59034
Pu-241	0	0.9912	0.8935	0	0.95596	0.73535	1.69131
Pu-242	0	0.4283	0.4240	0	0.79696	0.31775	1.11471
Burnup, MWd/MT	0	27,037	0	0	27,037	27,037	27,037
Total Uranium	1000	963.9513	258.1209	734.6562	245.75773	715.13531	960.89304
U-235, Wt. Frac.	0.026	0.0064409	0.00711	0.026	0.00312308	0.0064408	0.0055923
Total Plutonium	0	7.3845	7.2229	0	5.02840	5.47841	10.50681
Frac. Fiss. Pu	0	0.704652	0.70106	0	0.58496	0.70465	0.647367
Fraction Fissile	0.026	0.11749	0.026	0.026	0.014789	0.011749	0.0125338
U-236, Wt. Frac.	0	0.00334322	0	0	0.00077816	0.0033432	0.00268718

Table 19 (continued)

	4th Recycle of Plutonium				
	Charged		Discharged		
Isotope	Mixed Oxide	2.6 wt % Slightly Enriched	Mixed Oxide	2.6 wt % Slightly Enriched	Total
U-235	2.50381	16.50363	1.16887	3.94100	5.10987
U-236	0	0	0.25757	2.04562	2.30319
U-238	349.64924	618.25126	343.46758	605.88617	949.35375
Pu-239	5.55159	0	3.05765	2.67378	5.73143
Pu-240	3.06842	0	2.07670	1.11253	3.18923
Pu-241	1.97705	0	1.65863	0.62917	2.28780
Pu-242	2.49501	0	2.81517	0.27187	3.08704
Burnup, MWd/MT	0	0	27,037	27,037	27,037
Total Uranium	352.15305	634.75488	344.89402	611.87279	956.76681
U-235, Wt. Frac.	0.00711	0.026	0.00338907	0.0064408	0.0053408
Total Plutonium	13.09207	0	9.60815	4.98735	14.29550
Frac. Fiss. Pu	0.5750538	0	0.49086	0.70465	0.560961
Fraction Fissile	0.0274673	0.026	0.016601	0.011749	0.0135203
U-236, Wt. Frac.	0	0	0.00074681	0.0033432	0.00240726

result of the buildup of higher, nonfissile plutonium isotopes. Mixed oxide is seen to provide about 35% of the fissile requirements of the reload batch.

7.2 Financial Study

S. G. Ledford and J. D. McGaugh (ORGDP)

As input to the LWR Recycle Project--in particular, the LWR fuel cycle economics studies--some financial considerations were examined. One task involves examination of the capital structure of several large companies in various industries. Two of these, the petroleum and nuclear suppliers industries with their respective companies, are shown in Tables 20 and 21. Assets and stockholders' equity, as well as debt/equity ratios, are shown for each company included. Table 22 summarizes (by industry) long-term debt and equity in order to show general trends in the private sector. Information was obtained from Moody's Handbook of Common Stocks, 1976. This work is continuing. Early results were presented at a program status meeting at Savannah River Laboratory (SRL) on August 18.

7.3 Program Review

J. M. Morrison (ORGDP)

J. T. Bradbury, J. D. McGaugh, and J. M. Morrison participated in a meeting at SRL on August 18 to review the overall program of work on the LWR Economic Studies. Results to date, as well as the schedule of planned UCC-ND study topics, were presented. Similar presentations were made by personnel from SRL, SRP, HEDL, and PNL.

Table 20. Capitalization by companies

(Petroleum industry)

Company	Assets (Billions)	Stockholder's Equity (Billions)	D/E
Atlantic Richfield	7.4	3.7	0.44
Continental Oil	5.2	2.1	0.42
Exxon	22.8	17.0	0.19
Gulf Oil	12.4	6.4	0.20
Mobil Oil	15.0	6.8	0.27
Phillips Petroleum	4.5	2.4	0.37
Shell	7.0	3.9	0.31
Standard Oil (California)	12.9	6.5	0.21
(Indiana)	9.8	5.6	0.31
(Ohio)	4.2	1.5	1.35
Texaco	17.3	8.7	0.26
Union Oil (California)	3.8	1.9	0.40

Table 21. Capitalization by companies

(Nuclear reactor suppliers)

Company	Assets (Billions)	Stockholder's Equity (Billions)	D/E
Babcock & Wilcox	1.1	0.37	0.46
Combustion Engineering	1.0	0.36	0.27
General Electric	9.8	4.1	0.25
Westinghouse	4.9	2.0	0.32

Table 22. Capitalization by industry

Industry	Long-Term Debt (%)	Equity (%)	D/E
Petroleum	26.1	73.9	0.35
Chemicals	27.9	72.1	0.39
Metals and Mining	30.9	69.1	0.45
Auto/Defense	30.9	69.1	0.45
Nuclear Reactor Suppliers	24.2	75.8	0.32
Utilities	55.6	44.4	1.25

8. RADIOLOGICAL TECHNIQUES FOR ENVIRONMENTAL IMPACT ASSESSMENTS OF THE LWR FUEL CYCLE

D. C. Kocher and R. E. Moore (Environmental Sciences Division, ORNL)

8.1 Introduction

In estimating radiation doses to the population resulting from the release of radioactive materials to the atmosphere, it is usually assumed that man spends 100% of his time located 1 m above a smooth, infinite plane so that the only protection against airborne and ground-deposited radionuclides is provided by absorption of the radiations by air.

The assumption of continuous out-of-doors residence by man is clearly unrealistic. One study has concluded that the population spends at least 70% of the time in an indoor environment.[19] The largely indoor environment for the population may result in substantial reductions in radiation doses. The purpose of this project is to develop a methodology to estimate the radiological protection afforded by building structures inside which the population spends most of its time. The methodology is to be applied to radionuclides routinely released during the LWR fuel cycle.

8.2 Effect of Building Structures on Radiation Exposure Pathways

In general, we consider the radiation dose to man to be divided as follows:

1. Internal dose from inhaled radionuclides
2. External dose
   (1) Airborne radionuclides
   (2) Surface-deposited radionuclides

We do not consider other pathways, such as ingestion and exposure to contaminated water, for which the dose to man is not affected by building structures.

The internal dose from inhaled radionuclides is proportional to the airborne density of the radionuclides. Therefore, the effect of building structures on internal dose reduces simply to consideration of the effect of building structures on the concentration of airborne radionuclides.

For the case of external dose from airborne radionuclides, a building structure provides two kinds of protection. One is a reduction in dose resulting from a reduction in the airborne density of radionuclides inside the structure. The other is a reduction in dose resulting from the attenuation of gamma rays originating from radionuclides outside the structure. These two types of protection also apply to the case of external dose from surface-deposited radionuclides, where we consider the dose from radionuclides deposited on inside surfaces of the structure and the attenuation of gamma rays originating from radionuclides deposited on surfaces outside the structure.

For each of the three pathways considered, the effect of building structures on the radiation dose is described quantitatively by a so-called dose-rate protection factor, which is the ratio of the dose rate inside a structure to the corresponding dose rate with no structure present.

8.3 Model for Internal Dose Protection Factor

We assume a steady-state condition in which the airborne density for a given radionuclide is constant with time. The dose-rate protection factor

for internal dose is given by the ratio of indoor-to-outdoor air concentration. Using methods similar to the derivation of Eq. (7.84) of ref. 20, we have derived the following equation for the protection factor:

$$PF_{internal} = \frac{\lambda_v(1 - e^{-\lambda_a t})}{\lambda_a}, \qquad (1)$$

where

λ_v = air ventilation rate,

t = time,

$\lambda_a = \lambda_v + (V_{df}S_f + V_{dw}S_w + V_{dc}S_c)/V_h + \lambda$,

λ = radioactive decay constant,

V_{df}, V_{dw}, V_{dc} = deposition velocities of radioactive material on floor, walls, and ceiling,

S_f, S_w, S_c = surface areas of floor, walls, and ceiling,

V_h = volume of structure.

From a survey of available data,[21] recommended air ventilation rates are in the range λ_v = 0.5 to 1.5 hr^{-1}. Very little appears to be known about deposition velocities of particulates on inside surfaces of buildings. A general theoretical treatment of dry deposition processes combined with wind-tunnel experiments[22,23] and experiments for certain vapors[24] indicate deposition velocities inside a building as large as 0.1 to 0.25 cm-sec^{-1}, which is about a factor of 3 to 10 less than typical values for outdoor ground deposition velocities.

8.4 Model for External Dose Protection Factor

We consider the external dose rate from photons only. External dose rates with and without a building structure present are calculated using the so-called point-kernel integration method. We assume uniformly distributed radionuclides in the atmosphere and on the ground. Using Eq. (1) of ref. 25, we calculate the absorbed dose rate in air at any point from a specified volume (v) of airborne radionuclides as:

$$D_v = kS_v \sum_i \left[\frac{\mu_{en,i}}{\rho}\right] f_i E_i \int_v \frac{1}{4\pi r^2} B_{en}(\mu_i r)\, e^{-\mu_i r}\, dV \,, \qquad (2)$$

where

D_v = absorbed dose rate, rad/sec,

$k = 1.60 \times 10^{-8}$ g-rad-MeV^{-1},

$\mu_{en,i}$ = linear energy-absorption coefficient for ith photon in air, cm^{-1},

ρ = density of air, g/cm^3,

f_i = intensity of ith photon, number per disintegration,

S_v = source strength, dis cm^{-3} sec^{-1},

E_i = energy of ith photon, MeV,

r = distance, cm,

μ_i = linear attenuation coefficient for ith photon in air, cm^{-1},

B_{en} = energy-absorption buildup factor.

The integral extends over the volume of interest. The summation is over the photons emitted by the radionuclide.

If we assume a constant rate of deposition of radionuclides on surfaces, we calculate the absorbed dose rate in air at any point from a specified surface (s) of deposited radionuclides as:

$$D_s(t) = \frac{kF_s}{\lambda}\left(1 - e^{-\lambda t}\right) \sum_i \left[\frac{\mu_{en,i}}{\rho}\right] f_i E_i \int_s \frac{1}{4\pi r^2} B_{en}(\mu_i r)\, e^{-\mu_i r}\, dS \ , \quad (3)$$

where

t = time, sec,

F_s = source strength deposition rate, (dis sec^{-1})-cm^{-2}-sec^{-1}

λ = radioactive decay constant, sec^{-1}.

The other quantities are the same as in Eq. (2). The integral extends over the surface of interest.

External dose-rate protection factors for photon radiation from airborne and surface-deposited radionuclides are obtained by evaluating Eqs. (2) and (3) with and without a building structure present and taking the ratios of the resulting dose rates.

8.5 Implementation of the Models for Dose-Rate Protection Factors

In this section, we discuss the approximations and assumptions used in applying Eqs. (1)-(3) to specific dose-rate protection factor calculations.

8.5.1 Internal dose

The internal dose-rate protection factor [Eq. (1)] is explicitly time dependent. We choose to calculate a conservative estimate for the protection

factor by setting $(1 - e^{-\lambda_a t}) \equiv 1$, which is a good approximation for most radionuclide half-lives of interest. Therefore, the protection factor becomes

$$PF_{internal} = \lambda_v/\lambda_a \,, \tag{4}$$

a quantity depending only on the air ventilation rate, radioactive decay constant, building geometry, and deposition velocities on inside surfaces of the building structure.

8.5.2 External dose from airborne radionuclides

With no building structure present, we evaluate Eq. (2) for a uniform distribution of radionuclides over a hemispherical volume of infinite radius. The unprotected dose rate becomes:

$$D_{v,o} = \frac{kS_v}{2\rho} \sum_i \mu_{en,i} f_i E_i \int_o^\infty B_{en}(\mu_i r)\, e^{-\mu_i r} \,. \tag{5}$$

In order to evaluate the integral, we use the approximate Berger form of the buildup factor,[26] which is given by

$$B_{en}(\mu_i r) = 1 + C_i\, \mu_i r\, e^{D_i \mu_i r} \,. \tag{6}$$

The values of the coefficients C_i and D_i, which are dependent on the photon energy E_i, were obtained by performing a linear least-squares fit to the energy-absorption buildup factors for air given in ref. 27. With this approximation, the unprotected dose-rate in air becomes:

$$D_{v,o} = \frac{kS_v}{2\rho} \sum_i \mu_{en,i}\, f_i E_i \cdot \frac{1}{\mu_1} \left[1 + \frac{C_i}{(D_i - 1)^2} \right] . \tag{7}$$

The values of the attenuation and absorption coefficients are obtained by interpolation of values given in refs. 28 and 29.

With a building structure present, we assume for simplicity that the structure is a hemispherical shell of radius a and thickness τ. The contribution to the protected dose rate from the volume inside the structure is obtained from Eqs. (4)-(6) by replacing the outside source strength S_v by the inside source strength $S_v\ (\lambda_v/\lambda_a)$ and changing the upper limit of the integral to the building radius a. Similarly, the contribution to the protected dose rate from the volume outside the structure is obtained from Eq. (5) by changing the lower limit of the integral to a. In addition, we approximate the buildup factor for the case of a two-layer medium (air and wall material) by the Bowman-Trubey form[30] given by:

$$B_{en}(\mu_{i,a}r,\ \mu_{i,w}\tau) = B_{en,a}(\mu_{i,a}r)\ B_{en,w}(\mu_{i,w}\tau)\ e^{-\mu_{i,w}\tau}$$

$$+\ B_{en,w}(\mu_{i,a}r + \mu_{i,w}\tau)\ (1 - e^{-\mu_{i,w}\tau})\ , \qquad (8)$$

where the subscripts a and w refer to air and wall material, respectively. By using Eq. (6) for both air and wall material, Eq. (5) can then be evaluated. We are using buildup factors for concrete,[31] wood,[27] and water[32] to approximate wall materials.

The evaluation of the two terms for the protected dose rate as described above is straightforward but somewhat lengthy. The results are not given here but will be documented in a future publication.

8.5.3 External dose from surface-deposited radionuclides

With no building structure present, we evaluate Eq. (3) for a uniform distribution of radionuclides over an infinite, smooth plane. If z is the

height of the reference position above the plane (usually 1 m for the standard man out-of-doors calculation), we obtain the following result from Eqs. (3) and (6):

$$D_{s,o}(t) = \frac{kF_s}{2\rho\lambda}(1 - e^{-\lambda T}) \sum_i \mu_{en,i} f_i E_i \left[\tilde{E}_1(\mu_i z) - \frac{C_i}{D_i - 1} e^{(D_i - 1)\mu_i z} \right] . \tag{9}$$

The quantity $\tilde{E}_1(\mu_i z)$ is the well-known first-order exponential integral

$$\tilde{E}_1(\mu_i z) \equiv \int_z^\infty \frac{1}{r} e^{-\mu_i r} dr , \tag{10}$$

for which accurate polynominal and rational approximations are known.[33]

With a building structure present, we consider protected dose-rate contributions from the following sources: (1) radionuclides deposited on the inside walls and ceiling of the structure, (2) radionuclides deposited on the floor, (3) radionuclides deposited on the ground outside the structure, and (4) radionuclides deposited on the roof of the structure. In evaluating terms (1) and (2), we assume that the structure is a hemispherical shell; to evaluate terms (3) and (4), we assume a right circular cylindrical shell for the structure. We ignore possible deposition of radionuclides on the outside vertical walls of the structure.

The four terms contributing to the protected dose rate can then be evaluated in a tedious but straightforward manner using Eqs. (3), (6), and (8). The simplifying choice of hemispherical or cylindrical building geometries permits all integrals to be evaluated in closed form except for first-order exponential integrals. For term (1) above, we replace F_s in

Eq. (3) by $S_v V_d$ (λ_v/λ_a), where the deposition velocity is assumed to be $V_d \equiv (V_{dw} + V_{dc})/2$ as defined in Eq. (1). In term (2), F_s is replaced by $S_v V_{df}$ (λ_v/λ_a). The deposition rate for the roof is assumed to be the same as for the ground. For terms (1) and (2), the explicit time dependence is retained as a free parameter to describe the frequency with which inside building surfaces are cleaned. For deposition outside the building, we normally assume t = 50 years. Again, the formulas for the various terms will be documented in a later publication.

8.6 Limitations of the Model

The calculated dose rates described in the previous section are based on numerous approximations and simplifying assumptions. Among the most important are: (1) assuming infinite, uniformly distributed radionuclides in the atmosphere and on the ground; (2) assuming simple building structure geometrics with uniform wall thickness; (3) applying buildup factors calculated for infinite homogeneous media to finite, nonhomogeneous media; and (4) the use of the Berger and Bowman-Trubey approximations for buildup factors. Therefore, we recognize that the calculations of absolute dose rates are inherently limited in their accuracy. However, the essence of this project is to calculate ratios of dose rates with and without a building structure present. In calculating such ratios, many of the errors in the individual dose rates will tend to cancel.[34] Therefore, we believe that the calculated dose-rate protection factors are considerably more accurate than the individual dose rates, and that the accuracy of our cal-

culations will be limited as much by uncertainties in input parameters such as surface deposition velocities and deposition rates as they are by the use of many approximations.

One important type of protection from external radiation is not included in our model. It is well known that natural ground roughness and terrain irregularities provide considerable protection from radionuclides deposited on the ground compared with the standard smooth surface. Values for the natural protection factor due to ground roughness found in the literature[34] range from 0.5 to 0.1; thus the effect is sizable. These effects can be included after protection factors due to building structures have been calculated.

8.7 Progress to Date and Future Plans

During the present quarter, we have developed the models for calculating dose-rate protection factors, derived the equations to obtain the dose rates for the various pathways considered, and written a computer code to perform the calculations. The computer code will be used to perform an analysis of the sensitivity of the calculated protection factors to the variation of the many input parameters involved. Only a few preliminary calculations have been performed while the computer code is being tested and finalized. One important result evident thus far is that the overall protection factor for external dose from airborne plus ground-deposited radionuclides is very sensitive to the ratio of the airborne source strength S_v to the ground deposition rate F_s.

9. REFERENCES

1. C. D. Watson, B. C. Finney, G. A. West, and B. A. Hannaford, The Shear-Leach Process, Oak Ridge National Laboratory, 12-minute color movie, in sound (with summary data), ERDA Catalogue No. 0339, produced by S. Sinichak and E. C. Sienknecht (1963).
2. M. J. Bell, ORIGEN - The ORNL Isotope Generation and Depletion Code, ORNL-4828 (May 1973).
3. J. S. Watson, Heat Transfer from Spent Reactor Fuels During Shipping: A Proposed Method for Predicting Temperature Distribution in Fuel Bundles and Comparison with Experimental Data, ORNL-3439 (May 1963).
4. D. E. Metheny, Computer Program JACK, Bartlett-Snow and Co. (July 31, 1969).
5. B. L. Vondra, LWR Fuel Reprocessing and Recycle Program Quarterly Report for Period January 1 to March 31, 1976, ORNL/TM-5447 (May 1976).
6. B. L. Vondra, LWR Fuel Reprocessing and Recycle Program Quarterly Report for Period April 1 to June 30, 1976, ORNL/TM-5547 (July 1976).
7. K. Jones, "Nitrogen," p. 272 in Comprehensive Inorganic Chemistry, Vol. 2, ed. by J. C. Bailar, H. J. Emeleus, R. Nyholm, and A. F. Trotman-Dickenson, Pergamon, New York, 1973.
8. J. M. McKibben and J. C. Bercaw, DP-1248 (1971).
9. L. F. Audrieth and B. A. Ogg, "Oxidation of Hydrazine," pp. 115-52 in The Chemistry of Hydrazine, Chap. 6, Wiley, New York, 1951.
10. C. S. Schlea, M. R. Caverly, H. E. Henry, and W. J. Jenkins, DP-808 (1963).

11. J. I. Bryand and H. Rosenwasser, J. Chem. Educ. 39, 296 (1962).

12. V. S. Koltunov and V. I. Marchenko, Kinet. Catal. (USSR) 7, 202 (1966).

13. V. S. Koltunov, V. A. Nikolskii, and Yu. P. Agureev, Kinet. Catal. (USSR) 3, 764 (1962).

14. J. L. Swanson, BNWL-1584 (1971).

15. R. Huq and M. A. Nawab, Sci. Res. (Dacca, Pakistan) 5, (1968).

16. J. van R. Smit, Chem. Ind., p. 2018 (Dec. 5, 1964).

17. K. Alcock, F. C. Bedford, W. H. Hardwick, and H. A. C. McKay, J. Inorg. Nucl. Chem. 4, 100 (1957).

18. R. F. Barry, The Revised LEOPARD Code--A Spectrum Dependent Non-Spatial Depletion Code, WCAP-2759 (March 1965) and WCAC-3269-26 (August 1968).

19. J. P. Robinson and P. E. Converse, Summary of U. S. Time Use Survey, Institute for Social Research, University of Michigan, Ann Arbor, Michigan (1966).

20. D. M. Slade (ed.), Meteorology and Atomic Energy 1968, TID-24190, U.S. Atomic Energy Commission (July 1968).

21. T. H. Handley and C. J. Barton, Home Ventilation Rates: A Literature Survey, ORNL-TM-4318 (September 1973).

22. G. A. Sehmel, "Particle Eddy Diffusivities and Deposition Velocities for Isothermal Flow and Smooth Surfaces," J. Aerosol Sci. 4, 125 (1973).

23. G. A. Sehmel, "Particle Diffusivities and Deposition Velocities over a Horizontal Smooth Surface," J. Colloid Interface Sci. 37, 891 (1971).

24. W. F. Megaw, "The Penetration of Iodine into Buildings," Intern. J. Air Water Pollut. 6, 121 (1962).

25. M. L. Berger, "Energy Deposition in Water by Photons from Point Isotropic Sources," J. Nucl. Med. Suppl. No. 1, 15 (1968).

26. D. K. Trubey, A Survey of Empirical Functions Used to Fit Gamma-Ray Buildup Factors, ORNL-RSIC-10 (February 1966).

27. F. H. Clark, "Gamma-Ray Buildup Factors for Sand, Air, and Wood (Cellulose)," Nucl. Appl. 6, 588 (1969).

28. Radiological Health Handbook, U.S. Department of Health, Education, and Welfare, p. 137 (January 1970).

29. R. G. Jaeger (ed.), Engineering Compendium on Radiation Shielding, Vol. 1, p. 183, Springer-Verlag, New York, 1968.

30. D. K. Trubey, "Kernel Methods for Radiation Shielding Calculations," Nucl. Eng. Design 13, 423 (1970).

31. F. H. Clark and D. K. Trubey, "Energy and Dose Buildup Factors for Various Concretes," Nucl. Appl. 4, 37 (1968).

32. H. Goldstein and J. E. Wilkins, Jr., Calculations of the Penetration of Gamma Rays, NYO-3075 (1954).

33. M. Abramowitz and I. A. Segun (eds.), Handbook of Mathematical Functions, Dover Publications, New York (1965).

34. Z. G. Burson and A. E. Profio, Structure Shielding from Cloud and Fallout Gamma Ray Sources for Assessing the Consequences of Reactor Accidents, EGG-1183-1670 (December 1975).

INTERNAL DISTRIBUTION

1. S. I. Auerbach
2. Myer Bender
3. M. R. Bennett
4. J. O. Blomeke
5. W. D. Bond
6. B. F. Bottenfield
7. J. T. Bradbury, ORGDP
8. R. E. Brooksbank
9. C. H. Brown
10-14. W. D. Burch
15. S. R. Buxton
16. D. O. Campbell
17. J. M. Chandler
18. W. E. Clark
19. L. T. Corbin
20. D. J. Crouse
21. F. L. Culler
22. R. G. Donnelly
23. M. J. Feldman
24. D. E. Ferguson
25. L. M. Ferris
26. R. B. Fitts
27. E. L. Gaden, Jr. (Consultant)
28. E. H. Gift, ORGDP
29. J. H. Goode
30. N. R. Grant
31. W. S. Groenier
32. D. C. Hampson
33. G. S. Hill
34. D. E. Horner
35. A. R. Irvine
36. S. V. Kaye
37. A. D. Kelmers
38. C. E. Lamb
39. R. E. Leuze
40. J. C. Mailen
41. A. P. Malinauskas
42. Leon Maya
43. J. D. McGaugh, ORGDP
44. R. E. Moore
45. J. M. Morrison, ORGDP
46. E. L. Nicholson
47. A. R. Olsen
48. J. H. Pashley, ORGDP
49. F. L. Peishel
50. Herman Postma
51. R. H. Rainey
52. R. B. Richards (Consultant)
53. C. R. Richmond
54. H. C. Savage
55. A. C. Schaffhauser
56. C. D. Scott
57. R. G. Stacy
58. M. J. Stephenson, ORGDP
59. W. G. Stockdale
60. O. K. Tallent
61. L. M. Toth
62. H. E. Trammell, ORGDP
63. D. B. Trauger
64. W. E. Unger
65. V. C. A. Vaughen
66-75. B. L. Vondra
76. C. D. Watson
77. J. R. Weir, Jr.
78. M. E. Whatley
79. R. G. Wymer
80. O. O. Yarbro
81. Central Research Library
82. ORNL - Y-12 Technical Library Document Reference Section
83-87. Laboratory Records
88. Laboratory Records, ORNL R. C.
89. ORNL Patent Office
90. Nuclear Safety Information Center

EXTERNAL DISTRIBUTION

91. R. C. Adkins, Technical Representative, NUSAC, 777 Leesburg Pike, Falls Church, VA 22043
92. Aeroject Nuclear Company, 550 2nd Street, Idaho Falls, ID 83401
93. H. M. Agnew, Director, Los Alamos Scientific Laboratory, P. O. Box 1663, Los Alamos, NM 87545

94. T. W. Ambrose, Director, Pacific Northwest Laboratory, P. O. Box 999, Richland, WA 99352
95. C. K. Anderson, Combustion Engineering Nuclear Power Division, 1000 Prospect Hill Road, Windsor, CT 06095
96. F. H. Anderson, General Manager, Allied Chemical Corporation, 550 Second Street, Idaho Falls, ID 83401
97. Argonne National Laboratory, P. O. Box 2528, Idaho Falls, ID 83401
98. Argonne National Laboratory, 9700 South Cass Avenue, Argonne, IL 60439
99. J. F. Bader, Manager, Plutonium Recycle Fuel Programs, Westinghouse Electric Corporation, Box 355, Pittsburgh, PA 15230
100. F. P. Baranowski, Division of Nuclear Fuel Cycle and Production, U. S. Energy Research and Development Administration, Washington, DC 20545
101. R. G. Barnes, Manager, Technical Development, Advance Engineering, General Electric Company, 175 Curtner Avenue, San Jose, CA 95125
102. Battelle-Columbus Laboratories, 505 King Avenue, Columbus, OH 43201
103. R. C. Baxter, President, Allied-General Nuclear Services, P. O. Box 847, Barnwell, SC 29812
104. M. Binstock, Kerr-McGee Nuclear Corporation, Kerr-McGee Building, Oklahoma City, OK 73102
105. K. Bowlman, General Electric Company, 175 Curtner Avenue, San Jose, CA 95125
106. R. G. Bradley, Division of Nuclear Fuel Cycle and Production, U. S. Energy Research and Development Administration, Washington, DC 20545
107. M. G. Britton, Manager Technical Liaison, Corning Glass Works, Corning, NY 14830
108. J. Carp, Director for Energy Policy, Edison Electric, 90 Park Avenue, New York, NY 10016
109. W. T. Cave, Director, Monsanto Research Corporation, Mound Laboratory, P. O. Box 32, Miamisburg, OH 45332
110. B. H. Cherry, Manager of Fuel Resources, GPU Services Corporation, 260 Cherry Hill Road, Parsippany, NJ 07054
111. G. R. Corey, Vice Chairman, Commonwealth Edison Company, P. O. Box 767, Chicago, IL 60690
112. R. G. Cross, DBM Corporation, 1920 Alpine Avenue, Vienna, VA 22180
113. R. Cunningham, Nuclear Materials Safety and Safeguards, Nuclear Regulatory Commission, Washington, DC 20545
114. R. L. Dickeman, President, Exxon Nuclear Company, Inc., 777 - 106th Avenue, NE, Bellevue, WA 98004
115. Electric Power Research Institute, P. O. Box 10055, Palo Alto, CA 94303
116. R. Fullwood, Science Applications, Inc., 2680 Hanover Street, Palo Alto, CA 94303
117. R. L. Grant, Director of Nuclear Projects, Boeing Engineering and Construction Division, P. O. Box 3707, Seattle, WA 98124
118. Hanford Engineering Development Laboratory, Associate Lab Director, P. O. Box 1970, Richland, WA 99352
119. T. B. Hindman, Jr., Director, Fuel Cycle Project Office, U. S. Energy Research and Development Administration, Savannah River Operations Office, P. O. Box A, Aiken, SC 29801

120. A. H. Hines, Jr., President, Florida Power Corporation, P. O. Box 14042, St. Petersburg, FL 33733
121. C. A. Hirenda, Director of Marketing, Proposal Management, Inc., 121 N. Orionna Street, Philadelphia, PA 19106
122. P. Hogroian, Division of Nuclear Fuel Cycle and Production, U. S. Energy Research and Development Administration, Washington, DC 20545
123. R. Hoskins, Tennessee Valley Authority, 217 Electric Power Board Building, Chattanooga, TN 37401
124. C. H. Ice, Director, Savannah River Laboratory, E. I. du Pont de Nemours and Company, Aiken, SC 29801
125. R. H. Ihde, Manager, Contracts and Marketing, Babcock and Wilcox, P. O. Box 1260, Lynchburg, VA 24505
126. W. Johnson, Vice-President, Yankee Atomic Electric Company, 20 Turnpike Road, Westboro, MA 01581
127. W. A. Kalk, Manager, Nuclear Power Systems, Holmes and Narver, Inc., 400 East Orangethorne Avenue, Anaheim, CA 92801
128. M. I. Kaparstek, Manager of Proposals, Burns and Roe, Industrial Services Corporation, P. O. Box 663, Paramus, NJ 07652
129. K. Killingstad, Cont. Services, Battelle-Human Affairs Research Centers, 4000 N. E. 41st Street, Seattle, WA 98105
130. H. Kouts, Nuclear Regulatory Commission, Washington, DC 20545
131. C. Kuhlman, Division of Nuclear Fuel Cycle and Productions, U. S. Energy Research and Development Administration, Washington, DC 20545
132. J. A. Kyger, Associate Director, Argonne National Laboratory, 9700 South Cass Avenue, Argonne, IL 60439
133. F. W. Lewis, President, Middle South Utilities, Inc., Box 61005, New Orleans, LA 70161
134. W. H. Lewis, Nuclear Fuel Services, 6000 Executive Blvd., Rockville, MD 20952
135. J. L. Liverman, Division of Biomedical and Environmental Research, U. S. Energy Research and Development Administration, Washington, DC 20545
136. H. E. Lyon, Division of Safeguards and Security, U. S. Energy Research and Development Administration, Washington, DC 20545
137. L. W. Nelms, Chief, Research Branch, Research and Technical Division, Todd Company, P. O. Box 1600, Galveston, TX 77550
138. R. I. Newman, Vice President, Allied-General Nuclear Services, P. O. Box 847, Barnwell, SC 29812
139. R. D. Oldenkamp, Rockwell International, Atomics International Division, 8900 De Soto Avenue, Canoga Park, CA 91304
140. D. T. Pence, Science Applications, Inc., 1200 Prospect Street, P. O. Box 2351, La Jolla, CA 92038
141. G. B. Pleat, Division of Nuclear Fuel Cycle and Production, U. S. Energy Research and Development Administration, Washington, DC 20545
142. G. K. Rhode, Vice-President-Engineer, Niagara Mohawk Power Corporation, 300 Erie Boulevard, West, Syracuse, NY 13202
143. L. M. Richards, Nuclear Commercial Development Coordinator, Atlantic Richfield Company, Box 2679 - TA, Los Angeles, CA 90071
144. R. W. Roberts, Assistant Administrator for Nuclear Energy, U. S. Energy Research and Development Administration, Washington, DC 20545

145. J. Shefeik, General Atomic Company, P. O. Box 81608, San Diego, CA 92138
146. N. F. Seivering, Jr., Assistant Administrator for International Affairs, U. S. Energy Research and Development Administration, Washington, DC 20545
147. L. E. Smith, Manager-Fuel, Carolina Power and Light Company, P. O. Box 1551, Raleigh, NC 27602
148. D. Spurgeon, Division of Nuclear Fuel Cycle and Production, U. S. Energy Research and Development Administration, Washington, DC 20545
149. A. Squire, Director, Hanford Engineering Development Laboratory, P. O. Box 1970, Richland, WA 99352
150. C. Stephens, Virginia Electric Power Company, Nuclear Fuel Service Department, 512 Franklin Building, P. O. Box 26666, Richmond, VA 32361
151. N. Stetson, Manager, U. S. Energy Research and Development Administration, Savannah River Operations Office, P. O. Box A, Aiken, SC 29810
152. S. Stoller, Western Reprocessors, The S. M. Stoller Corporation, 1250 Broadway, New York, NY 10001
153. K. Street, Associate Director, Lawrence Radiation Laboratory, P. O. Box 808, Livermore, CA 94550
154. G. Stukenbroeker, NL Industries, P. O. Box 928, Barnwell, SC 29812
155. L. D. Tokerud, Vice-President, Aerojet Energy Conversion Company, 1120 Connecticut Avenue, NW, Suite 1050, Washington, DC 20036
156. Dr. Uhrig, Florida Power and Light Company, P. O. Box 013100, Miami, FL 33101
157. E. J. Wahlquist, Deputy Assistant Director for Terrestrial Programs, U. S. Energy Research and Development Administration, Washington, DC 20545
158. D. S. Webster, Argonne National Laboratory, Building 205, 9700 South Cass Avenue, Argonne, IL 60439
159. A. K. Williams, Director, Nuclear Technology Division, Allied-General Nuclear Services, P. O. Box 847, Barnwell, SC 29812
160. U. S. Energy Research and Development Administration, Chicago Operations Office, Contracts Division, 9800 South Cass Avenue, Argonne, IL 60439
161. U. S. Energy Research and Development Administration, Division of RDD, Energy Systems Analysis, Washington, DC 20545
162. U. S. Energy Research and Development Administration, Division of RDD, Engineering and Technology, Washington, DC 20545
163. U. S. Energy Research and Development Administration, Division of RDD, LMFBR Programs, Washington, DC 20545
164. U. S. Energy Research and Development Administration, Division of RDD, Reactor Safety, Washington, DC 20545
165. U. S. Energy Research and Development Administration, Library, Washington, DC 20545
166. U. S. Energy Research and Development Administration, Research and Technical Support Division, P. O. Box E, Oak Ridge, TN 37830
167. U. S. Energy Research and Development Administration, Oak Ridge Operations Office, Reactor Division, P. O. Box E, Oak Ridge, TN 37830
168. U. S. Energy Research and Development Administration, Patent Office, Washington, DC 20545

169. U. S. Energy Research and Development Administration, Richland Operations Office, P. O. Box 550, Richland, WA 99352
170. U. S. Energy Research and Development Administration, Southern California Energy Program Office, P. O. Box 1446, Canoga Park, CA 91304
171. U. S. Energy Research and Development Administration, Technical Information Center, Oak Ridge, TN 37830
172. U. S. Energy Research and Development Administration, Division of Reactor Development Demonstration, Washington, DC 20545
173. U. S. Energy Research and Development Administration, Idaho Operations Office, 550 2nd Street, Idaho Falls, ID 83401
174. U. S. Energy Research and Development Administration, Nevada Operations Office, P. O. Box 14100, Las Vegas, NV 89114
175. U. S. Energy Research and Development Administration, San Francisco Operations Office, 1333 Broadway, Wells Fargo Building, Oakland, CA 94612

☆ U.S. GOVERNMENT PRINTING OFFICE: 1976-748-189/27